A STUDY OF SEISMIC RESPONSE OF ROTATING MACHINES SUBJECTED TO MULTI–COMPONENT BASE EXCITATIONS

by

Tsu–Shen Chang and Mahendra P. Singh

Technical Report of Research Supported by
The National Science Foundation
Under Grant Number BCS–8822864

Department of Engineering Science and Mechanics
Virginia Polytechnic Institute and State University
Blacksburg, VA 24061–0219

May 1992

Engineering Report No. VPI–E–92–11

BIBLIOGRAPHIC DATA SHEET	1. Report No. VPI-E-92-11	2.	3. PB92-188135

4. Title and Subtitle

A STUDY OF SEISMIC RESPONSE OF ROTATING MACHINES SUBJECTED TO MULTI COMPONENT BASE EXCITATIONS

5. Report Date: MAY 1992

6.

7. Author(s)

8. Performing Organization Rept. No.

9. Performing Organization Name and Address

Department of Engineering Science and Mechanics
Virginia Polytechnic Institute and State University
Blacksburg, VA 24061-0219

10. Project/Task/Work Unit No.

11. Contract/Grant No.: BCS-8822864

12. Sponsoring Organization Name and Address

National Science Foundation
1800 G. Street, NW
Washington, DC 20550

13. Type of Report & Period Covered: TECHNICAL

14.

15. Supplementary Notes

ies,

16. Abstracts

The rotating machines like motors, generators, pumps and turbines are commonplace in modern industrial and power generation facilities. The failure of these machines during an earthquake can disrupt the functioning of these facility which can have serious operational and safety consequences. In this study, the response behavior of rotating machines subjected to random, multi-component base motions is examined. A response spectrum method is developed to calculate the seismic design response of machines for seismic inputs defined in terms of the base motion response spectra. The contributions of various terms in the equations of motion which complicate the response analysis are carefully evaluated to see if they can be eliminated to simplify the analysis. The numerical study shows that the contribution of the real eigenproperties of the machines can be ignored. Also, in most cases of a machine placed on the ground directly or installed in a building with torsional response, the effect of the rotational components of the input motion at the base of the machine can be ignored in the calculation of the machine response. However, in the cases where the rotational components are expected to be very strong, the proposed response spectrum approach can still be used.

17. Key Words and Document Analysis. 17a. Descriptors

Rotating Machines,
Turbines
Motors
Generators
Pumps
Earthquakes
Seismic Response,
Power Plants
Refineries
Chemical Plants
Vibrations, Dynamics
Modal Analysis
Damping, Frequency

17b. Identifiers/Open-Ended Terms

17c. COSATI Field/Group

18. Availability Statement	19. Security Class (This Report)	21. No. of Pages
Unlimited Distribution	UNCLASSIFIED	109
	20. Security Class (This Page) UNCLASSIFIED	22. Price

Acknowledgements

This report is the M.S. thesis of Tsu-Sheng Chang, which was submitted to the faculty of the Virginia Polytechnic Institute and State University in partial fulfillment of the requirements for the degree Master of Science in Engineering Mechanics, with M. P. Singh as the thesis advisor.

This work was financially supported by the National Science Foundation through Grant Number BCS-8822864 with Dr. S. C. Liu as its Program Director. This financial support is gratefully acknowledged. The opinions, findings and conclusions or recommendations expressed in this report are those of the writers and these do not necessarily reflect the views of the National Science Foundation.

A Study of Seismic Response of Rotating Machines Subjected to Multi-Component Base Excitation

by

Tsu-Sheng Chang

Committee Chairman: M. P. Singh

Engineering Science and Mechanics

(ABSTRACT)

Rotating machines such as motors, generators, turbines, etc. are crucial mechanical components of modern industrial and power generation facilities. For proper functioning of these facilities during and after an earthquake, it is essential that the rotating machines in these facilities also function as desired. The dynamics of a rotating machine is quite complex. It is further complicated by the presence of earthquake induced base motions. The response spectrum methods, which are now commonly used for calculating seismic design response of civil structures, can not be used as such for calculating the design response of rotating machines. In this thesis, a response spectrum method which can be applied to the rotating machines is develpoed.

To develop the response spectrum approach, a generalized modal superposition method is utilized. The random vibration analysis is applied to incorporate the

stochastic characteristics of the seismic inputs. The applicability of the proposed response spectrum approach is verified by a simulation study where fifty sets of acceleration time histories are used. The proposed method considers the fact that earthquake induced base motions have several components, including rotational inputs. To define the correlation between the rotational and translational input components of the excitation, the correlation matrix and a travelling seismic wave approaches are used. The numerical results are obtained to evaluate the effect of rotational input components on the response of a rotating machine. It is observed that the rotational components are important only when they are very strong. In actual practice, such strong rotational inputs are not expected to excite rotors which are either directly placed on ground or are placed in common buildings. In the proposed spectrum approach, nevertheless, the effect of rotational input components can be easily incorporated if the correlation between various excitation components is specified.

Table of Contents

List of Figures

List of Tables

Chapter 1

Introduction

Rotating machines such as pumps, generators, motors and turbines are crucial components frequently encountered in modern industrial and power generation facilities, and their operational performance has long been of major concern to engineers. Since quite often the failures of these equipments can have damaging consequences, especially in the nuclear power plants, chemical plants and emergency installations like hospitals, it is essential that they maintain proper functioning during and after the occurrence of an earthquake. The investigations of adequate designs are, therefore, necessary to ensure that these rotating machines in the structures located in seismically active areas can withstand earthquake induced excitations and meet critical demands.

The dynamic behavior of rotating systems has been a topic of interest to mechanical engineers for a long time, but it is only recently that increasing research effort has been devoted to their analysis for seismic loads. The dynamic characteristics of rotating machines under seismic loadings are quite different from those of the buildings, dams, pipings, etc. The seismic behavior of these latter systems has been

investigated quite exhaustively in the last two decades. For these systems, analytical methods utilizing design response spectra as seismic inputs have been developed to calculate the seismic design response under multi-component earthquakes. However, similar methods are not available currently for calculating the seismic design response of rotating machines. The primary objective of this work, therefore, is to develop a response spectrum approach for calculating the design response of rotating systems subjected to multi-component seismic excitations.

The rotating machines are quite complex dynamic systems to analyze. The equations of motion of these systems become especially more complicated when earthquake motions are involved. The foremost complexities in the dynamic analysis of these machines for earthquake motions arise from the presence of the (1) gyroscopic terms caused by the rotation of a rotor about its shaft, and (2) parametric terms caused by the rotational excitations at the base, in both the damping and stiffness matrices of the equations of motion. The forcing function terms in the equations of motion are also quite involved; they not only contain all six ground acceleration related inputs, but also contain terms which depend on the rotational velocity components of the base motion. In addition to all the above terms, there are also nonlinear terms in the form of products of the base velocities, which introduce further mathematical difficulties in the analysis. Fortunately, a previous study by Suarez et al. (1991) on the seismic response of rotor-bearing systems has observed that for earthquake induced ground motions the parametric terms in the system matrices of the equations of motion as well as the nonlinear terms in the inputs can be all neglected without causing any appreciable error in the calculated response of the system. This observation leads to significant simplifications in the development of an analytical method to calculate the seismic response of rotating machines.

The equations of motion for a rotating system are quite difficult to solve in their general form. In early studies, time history analyses which employed step-by step numerical techniques carried out in the time domain were used to compute the response. These kind of approaches, however, are quite cumbersome, expensive, and time consuming. A more efficient and reliable method is required. Here a response spectrum approach is presented to obtain the design response of rotating machines for seismic design inputs defined in terms of base motion response spectra. To utilize the base motion spectra in the analysis, it is necessary to characterize the dynamic properties of the rotating machines in terms of modal frequencies and damping ratios. Since the system matrices for rotating machines are not necessarily symmetrical, here a generalized modal approach is used to define the modal frequencies and damping ratios to be used in the response spectrum approach. In the development of the response spectrum approach, the stochastic characteristics of earthquake induced motions are incorporated through random vibration analysis.

The method includes the multiple components of the seismic inputs applied at the base of the machine. The input components considered in the study are: three translational accelerations, three rotational accelerations and three rotational velocities. They all can be correlated. Two methods of specifying the correlation between the excitation input components are considered. One method considers a travelling seismic wave model for machines sitting on the ground. The other utilizes a correlated floor spectra method, which is suitable for machines sitting on raised pedestals or for machines installed on building floors. In the travelling seismic wave model, the rotational components are expressed in terms of the translational accelerations. In the correlated floor spectra method, on the other hand, the correlation between various excitation components is directly defined through the correlation matrix. A

methodology is developed for each model to calculate the maximum response of the system.

Numerical results are obtained for a rotating system to demonstrate the applications of the proposed approach. The response spectrum method is verified by a time history simulation study. The contribution associated with the real eigenproperties of the system to the total response is also evaluated. Responses of the rotor under the rotational excitations of different intensities are presented to examine the effect of rotational inputs on the system response. Concluding remarks are provided in the end of this thesis along with some suggested future studies.

Chapter 2

Characteristics of Rotating Machines

2.1 Introduction

The subject of dynamics of rotating machines has been of continued research interest to mechanical engineers and there is abundance of literature devoted to the stability analysis of these machines. The research on the seismic response analysis of the rotating machines, however, is relatively more recent, and in the engineering literature there are some publications dealing with this subject now. See, for example, Asmis and Duff (1978), Iwatsubo et al. (1979), Srinivasan and Soni (1984), and Hori (1988).

A review of the early studies on seismic analysis of rotating machines is given by Srinivasan and Soni (1982). The first paper which considered the flexibility of the rotating shaft and the effect of the fluid film bearings on the response of rotating systems was by Srinivasan and Soni (1984). The seismic excitation inputs at the base included rotational as well as translational components. They developed the equations of motion by applying Newton's law combined with finite element discretization of the shaft. The linear interpolation functions were used to describe the displacement field

over a finite element. The equations of motion identified the presence of gyroscopic and parametric terms in the system matrices. Some numerical results obtained by a step-by-step numerical integration technique for the seismic input defined by a time history were also presented.

A more comprehensive study on the seismic behavior of rotating machines has been recently conducted by Suarez, Singh, and Rohanimanesh (1992). The flexibility of the shaft was considered by utilizing a Timoshenko beam model with shear deformation and rotatory inertia terms. The displacement field over a finite element was represented by cubic beam interpolation functions; the formulation was, however, general enough to enable the use of any other suitable interpolation functions. The stiffness and damping contributions of the supporting bearings were also included in the analysis. The variational approach with Hamilton's principle and Lagrange's equations was adopted to develop the equations of motion. In this research, we have used the equations of motion derived by Suarez et al (1992). Since these equations and the conclusions of their study are very relevant to this work, they are briefly described and reviewed in this chapter.

2.2 Equations of Motion

The equations of motion of a shaft-disk-bearing system in a finite element model can be written in the following standard form:

$$[M]\{\ddot{u}\} + [C]\{\dot{u}\} + [K]\{u\} = \{f(t)\} \tag{2.1}$$

where $[M]$, $[C]$, and $[K]$ are the mass, damping, and stiffness matrices respectively, $\{f(t)\}$ is the excitation vector, and $\{u\}$ is the vector of generalized nodal displacements measured relative to the base. All these system matrices and vectors are

assembled by the regular finite element analysis procedures over the rotor elements along the shaft. In the equations of motion, the stiffness and damping contributions from the bearing are imposed only at those nodes where the bearings are located. At each node, there are two translational (q_1,q_2) and two rotational degrees of freedom (q_3,q_4), as shown in Figure 2.1. Thus the total number of degrees of freedom of the system is four times the number of nodes. The axial displacements (u_z,θ_z) are not considered. The input base motion has three translational (x_b,y_b,z_b) and three rotational components (θ_{xb},θ_{yb},θ_{zb}), and all six appear in the forcing function $\{f\}$. Explicit expressions for $[M]$, $[C]$ and $[K]$ matrices and the excitation vector $\{f\}$ of a typical rotor element, as developed by Suarez et al (1992), are given in Appendix A of this thesis.

The mass matrix $[M]$ of the rotor system is symmetric, similar to the mass matrices usually encountered in common structural vibration problems. The damping and stiffness matrices $[C]$ and $[K]$, on the other hand, are quite different from those of the conventional structures. The damping matrix has a skew symmetric part consisting of the gyroscopic terms due to Coriolis effect from the shaft spinning and the parametric terms which depend on the rotational velocity inputs at the base. The other part of the damping matrix is symmetric and contains the damping coefficients coming from the fluid film bearings. These terms are similar to the viscous damping terms normally encountered in mechanical vibrations. These bearing terms are functions of physical parameters of the bearing as well as the spinning speed of the shaft. They provide desirable stability to the motion of the system. The stiffness matrix $[K]$ is as involved as the damping matrix. It has a constant symmetric part provided by the stiffness of the shaft and another symmetric but parametric terms involving the product of base rotational velocities. The asymmetric portion of the $[K]$ matrix

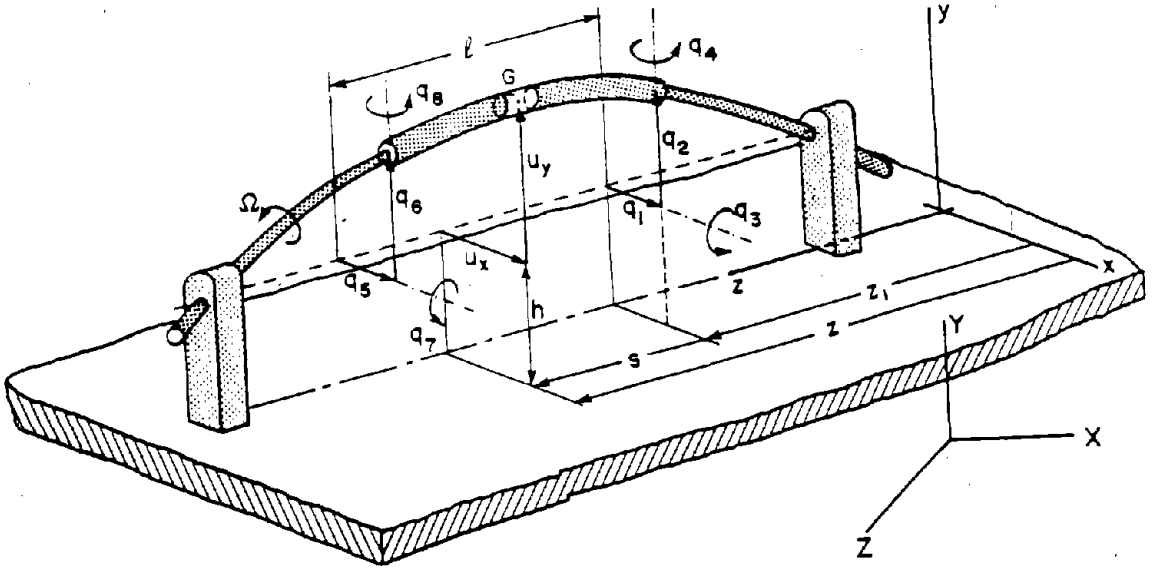

Figure 2.1: A schematic rotor with nodal coordinates and system of axes

has parametric terms from rotational accelerations and bearing-introduced stiffness coefficients. The spring forces in the x and y directions supplied by the bearings are coupled with each other and depend on the physical properties of the bearing and rotor spinning speed. However, the stiffness entries due to bearings in the system matrices are not symmetrical. This asymmetry causes instability in the shaft motion. It also complicates the solution of the equations of motion.

The forcing function term $\{f\}$ is interesting in its own way. It is quite different from the simple force vector appearing in the right hand side of the equation of regular structural and mechanical systems. Here, it is divided into four parts to get a closer inspection. The first part represents the commonly encountered terms associated with the translational accelerations. The second one depends on the rotational acceleration inputs at the base. The third part involves the base rotational velocity components combined with the spinning speed of the rotor, and the remaining one is a function of nonlinear input terms associated with both the translational and rotational velocity excitations at the foundation. The last part particularly is problematic from the point of view of using the response spectrum approach due to its nonlinearity. All these terms are identified in Appendix A.

2.3 Response Characteristics

The solution of the equations of motion given in equation (2.1) is quite involved primarily because of the presence of the parametric terms in the damping and stiffness matrices. Moreover, the complexities of the forcing function vector compound the mathematical operations. To compute the rotor response from the equations of

motion in their most general form, one will have to resort to a step-by-step numerical method. This kind of approach is, obviously, quite cumbersome for the design purposes since one has to carry out the procedures for several groups of possible design level ground motions. To obtain the design response, an analytical technique which will not require expensive and time consuming time history analysis would be preferred; nevertheless, this does not seem feasible as long as the parametric terms exist.

Suarez et al. (1992) performed a series of time history calculations by using the Newmark-β step-by-step integration method. The time histories of the seismic input motions at the base were generated by simulation for a Kanai-Tajimi type of ground spectral density function which is commonly used to represent seismic ground motions in the stochastic form. It was observed that there was essentially no change in the response when the parametric terms were eliminated from the damping and stiffness matrices. Even at quite strong levels of rotational excitations the magnitude and pattern of the response time histories showed little difference. This result leads to the following very important conclusion: the parametric terms in the formulation can be deleted from the system matrices without affecting the outcome. This assertion enables one to adopt the linear modal analysis to compute the seismic response of a rotor system and makes it possible to develop a response spectrum approach.

In their research on the response characteristics of the rotating machines Suarez et al. (1992) also investigated the effects of the nonlinear terms in the forcing function and base rotational inputs. They concluded that the contribution to the response from the nonlinear part in the excitations, which is due to the products of rotational velocities or rotational and translational velocities, is insignificant. These product

terms can be ignored in the analysis without noticeably influencing the response. This observation also greatly simplifies the random vibration analysis which is used in the derivation of the spectrum approach formulations. On the other hand, the rotational motions at the base might cause considerable differences in the rotor response depending on the intensity of these excitation components. Therefore, they should not be arbitrarily removed without an appropriate evaluation. However, the existence of the rotational accelerations and velocities does not pose any additional problems in the response spectrum approach. The studies on both the cases of including and excluding the rotational base motions are presented later in this thesis.

2.4 Rotor Stability

The prerequisite condition for performing any response analysis for a rotor system is that it has to be stable all the time. A dynamically unstable rotating machine when excited by earthquake induced motions will have sustainingly increasing response if the applied excitation persists (see Figure 2.2). Such a situation will definitely result in mechanical failures of the system. To ascertain the proper implementation of the analysis model one has to pay attention to the stability characteristics of the rotating machinery.

The stability of a rotating system is directly related to its spinning speed. Here the instability speed is defined as the spinning speed beyond which the response becomes unbounded. To obtain this instability speed we need to perform the eigenvalue analysis for the system at various spinning speeds. The complex eigenvalues of the system can be used to calculate the modal frequencies (ω_j) and modal damping ratios (β_j) as follows:

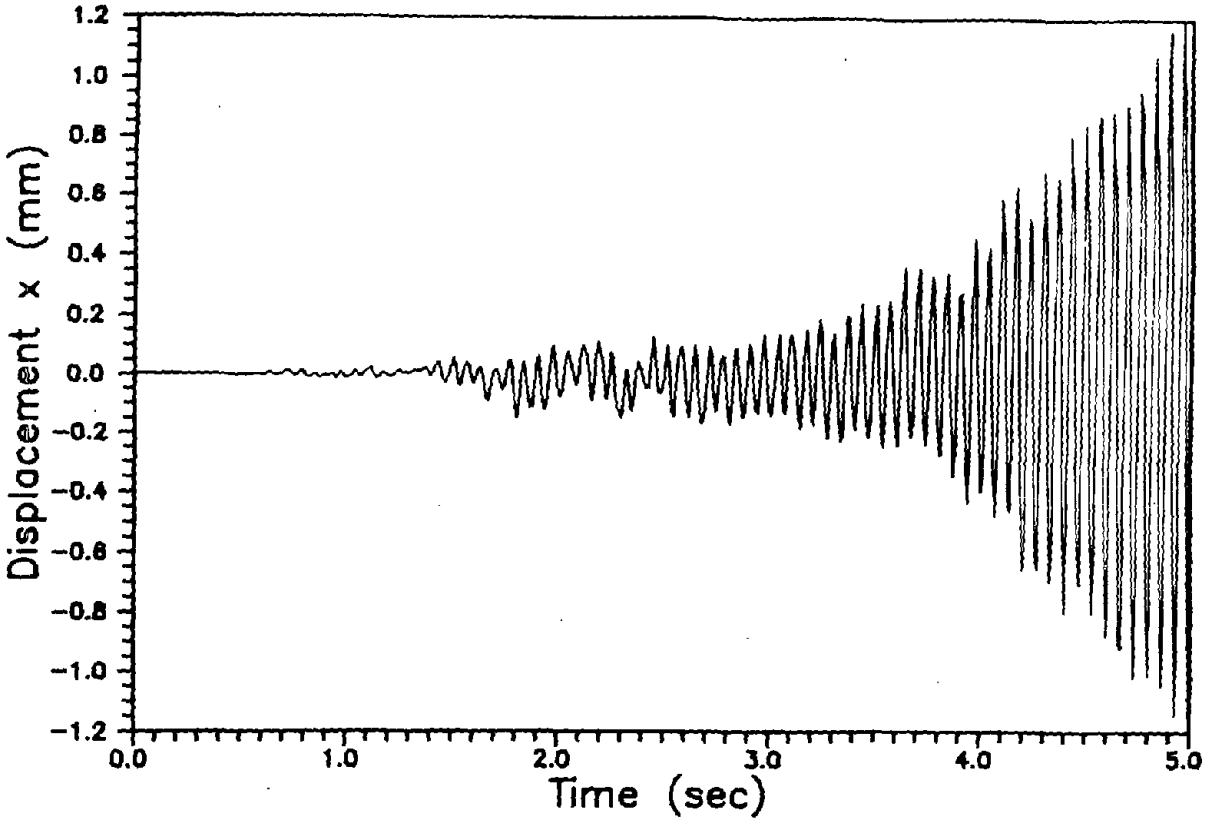

Figure 2.2: Unstable rotor response

$$\omega_j = |\lambda_j| \tag{2.2}$$

$$\beta_j = -\frac{Real(\lambda_j)}{\omega_j} \tag{2.3}$$

where λ_j is the eigenvalue of the jth mode. For a stable rotor system all the eigenvalues must have negative real parts, which also means that all modes should have positive damping ratios. A positive real part or negative damping ratio implies instability in the system. Thus to identify the instability speed one plots the algebraically largest real part of the eigenvalue against the spinning speed, as is done in Figure 2.3 for the example problem studied in this research. The point at which the curve intersects the zero axis provides the instability speed. As long as a rotor is operating below the instability speed, the response under seismic loads will be bounded.

In a finite element analysis of a rotor it has been indicated by Suarez et al. (1992) that the instability in a system can be masked by inappropriate use of interpolation functions with a finite element discretization scheme. It was shown that when the linear interpolation functions were used to model the deformation of a finite element, the instability did not show up until a large number of finite elements were considered. The cubic functions, on the other hand, showed the unstable behavior even with a few finite elements. Because the use of linear interpolation functions is misleading and inefficient, their use is not recommended for the analysis of rotating systems. In the numerical work here, therefore, the cubic interpolation functions have been used.

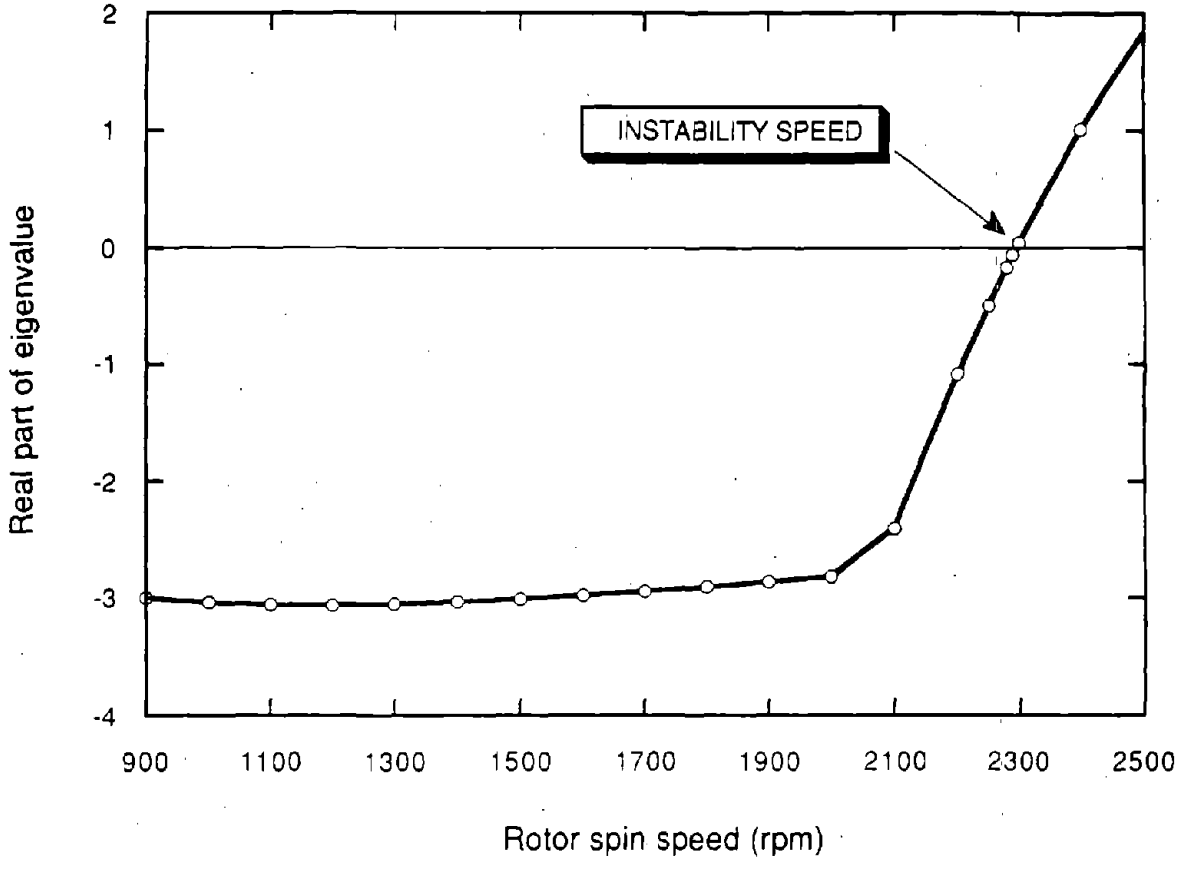

Figure 2.3: Determination of the instability speed

Chapter 3

Stochastic Formulation and Response Spectrum Analysis

3.1 Introduction

As indicated in the preceding discussions, the equations of motion of a rotating system, which are rather complicated to solve in their general form, can be simplified a great deal by deleting the problematic parametric and nonlinear terms without affecting the accuracy of the calculated response. Since these modified equations are linear, it is possible to develop a response spectrum approach to obtain the design response for rotating machines. In this chapter, the derivation of such response spectrum methods is presented for their use with multi-component seismic base excitations.

To use the seismic inputs defined in terms of base spectra, it is necessary that the modal frequencies and damping ratios of the system be identifiable. To accomplish this, here a generalized modal analysis approach, applicable to systems which have general asymmetric matrices in the equations of motion, is adopted. To include the correlation between the components of the base motion in the development of the

response spectrum approach, here two models have been considered. In the first method, the correlation between rotational and translational inputs is defined by using a travelling seismic wave model, earlier used by Ghafory-Ashtiany and Singh (1986). This correlation depends upon the direction of the upcoming seismic wave. Since this direction will not be known a priori, a procedure to calculate the worst-case response is presented. In the second model, the correlation matrix between the input excitations is defined directly either in terms of cross spectral density functions or in terms of cross response spectra of the components. In both models the effects of translational and rotational components have been seperated out. It is possible to include or ignore any of these input base motions in the calculation of the rotor response.

3.2 General Modal Analysis

The modified equations of motion for a rotor system subjected to seismic base excitations in a finite element model are rewritten in the following form:

$$[\bar{M}]\{\ddot{u}\} + [\bar{C}]\{\dot{u}\} + [\bar{K}]\{u\} = \sum_{i=1}^{n_e} \{\hat{f}(t)\}_i \tag{3.1}$$

The mass matrix $[\bar{M}]$ is the same as that given in equation (2.1), but $[\bar{C}]$ and $[\bar{K}]$ are the system damping and stiffness matrices without parametric terms. The vectors $\{\hat{f}\}_i$ on the right hand side comprise of only the linear input terms. In equation (3.1) the force vector is expressed as a sum of n_e terms representing inputs with different characteristics. The motivation behind this seperation of terms in the forcing function was to identify the effect of these different types of inputs in the response and evaluate their individual contributions.

Since $[\bar{C}]$ and $[\bar{K}]$ in equation (3.1) are general matrices without any symmetry, a generalized modal analysis approach is adopted to solve the vibration problem. In this approach equation (3.1) is rearranged in the state vector form as follows:

$$[A]\{\dot{y}\} + [B]\{y\} = \{F\} \tag{3.2}$$

where

$$[A] = \begin{bmatrix} [\bar{M}] & [\bar{C}] \\ 0 & [\bar{M}] \end{bmatrix}$$

$$[B] = \begin{bmatrix} 0 & [\bar{K}] \\ -[\bar{M}] & 0 \end{bmatrix}$$

$$\{y\} = \begin{Bmatrix} \{\dot{u}\} \\ \{u\} \end{Bmatrix}$$

$$\{F\} = \sum_{i=1}^{n_e} \begin{Bmatrix} \{\hat{f}\}_i \\ \{0\} \end{Bmatrix}$$

Note that the total degrees of freedom in the state space is $2n_t$ where n_t is the system degrees of freedom for the finite element rotor model. Also notice that neither of the matrices $[A]$ and $[B]$ is symmetric.

To decouple the equations of motion in (3.2), we need the solution of the following adjoint eigenvalue problems associated with the free vibration of the dynamic system defined:

$$\begin{aligned} [B]\{\psi_R\}_j &= -\lambda_j[A]\{\psi_R\}_j \\ [B]^T\{\psi_L\}_j &= -\lambda_j[A]^T\{\psi_L\}_j \end{aligned} \tag{3.3}$$

where $\{\psi_R\}_j$ and $\{\psi_L\}_j$ represent the right and left eigenvectors and λ_j the corresponding eigenvalue for the jth mode. The modal frequency and damping ratio can

be calculated from the eigenvalue by using equations (2.2) and (2.3). The right and left eigenvectors satisfy the following biorthonormality relationships with respect to matrices $[A]$ and $[B]$:

$$\begin{aligned} [\Psi_L]^T[A][\Psi_R] &= [I] \\ [\Psi_L]^T[B][\Psi_R] &= -[\Lambda] \end{aligned} \tag{3.4}$$

in which

$$\begin{aligned} [\Psi_R] &= [\{\psi_R\}_1, \{\psi_R\}_2, \cdots, \{\psi_R\}_{2n_t}] \\ [\Psi_L] &= [\{\psi_L\}_1, \{\psi_L\}_2, \cdots, \{\psi_L\}_{2n_t}] \\ [\Lambda] &= diag(\lambda_j) \end{aligned}$$

$[\Psi_R]$ and $[\Psi_L]$ are called right and left eigenvector matrices and $[\Lambda]$ is the diagonal matrix of eigenvalues. The first of equation (3.4) is used for normalizing the eigenvectors, one set or both, for mathematical convenience.

The state vector $\{y\}$ in equation (3.2) can be expressed as a linear combination of the right eigenvectors as:

$$\{y(t)\} = [\Psi_R]\{q(t)\} \tag{3.5}$$

where $\{q(t)\}$ is the vector of principal coordinates. By the substitution of equation (3.5) into equation (3.2), premultiplication of the resulting equation by $[\Psi_L]^T$, and finally imposition of the biorthonormality condition given in equation (3.4), we obtain the following uncoupled set of equations for the principal coordinates:

$$\{\dot{q}\} - [\Lambda]\{q\} = [\Psi_L]^T\{F\} \tag{3.6}$$

The jth equation of (3.6), which can be written as:

$$\dot{q}_j - \lambda_j q_j = \{\psi_L\}_j\{F\} \quad j = 1, 2, \ldots, 2n_t \ . \tag{3.7}$$

can be solved to define the principal coordinate q_j as follows:

$$q_j(t) = \int_0^t e^{\lambda_j(t-\tau)}\{\psi_L\}_j^T\{F(\tau)\}d\tau \tag{3.8}$$

In this solution, it is assumed that the system starts from rest.

Any response quantity $S(t)$ which is a linear function of the nodal displacements and velocities can always be defined as:

$$S(t) = \{T\}^T\{y(t)\} \tag{3.9}$$

where $\{T\}$ is the transformation vector of size $(2n_t \times 1)$. Generally speaking, almost all the fundamental response quantities that designers are interested in, such as the disk displacements, bearing forces, moments or dynamic stresses in the rotor shaft, are linearly related to the state vector $\{y\}$. The elements of the transformation vector $\{T\}$ depend upon the response quantity sought. They are defined in terms of the physical and mechanical properties of the system. Combining equations (3.5) and (3.9), we obtain:

$$S(t) = \sum_{j=1}^{2n_t}\{T\}^T\{\psi_R\}_j q_j(t) \tag{3.10}$$

The final form of the dynamic response by modal analysis thus can be written as follows:

$$S(t) = \sum_{j=1}^{2n_t}\{T\}^T\{\psi_R\}_j\{\psi_L\}_j^T\int_0^t e^{\lambda_j(t-\tau)}\{F(\tau)\}d\tau \tag{3.11}$$

To thoroughly explore the effect of various terms in the base inputs $\{F(t)\}$, the force vector is rearranged in the following way:

$$\{F(t)\} = \sum_{i=1}^{n_e}\begin{Bmatrix}\{\hat{f}\}_i \\ \{0\}\end{Bmatrix}$$

$$= \sum_{i=1}^{n_e} \{r\}_i E_i(t) = [r]\{E(t)\} \tag{3.12}$$

where $[r] = [\{r\}_1, \{r\}_2, \cdots, \{r\}_{n_e}]$, is the influence coefficient matrix of size $(2n_t \times n_e)$ formed by rotor constants; $\{E\} = \{E_1, E_2, \cdots, E_{n_e}\}^T$ is the vector of excitation components at the base. For the following three cases, this vector is defined as follows:

1. $n_e = 3$, when only the translational acceleration inputs are considered.

$$\{E\} = \{\ddot{x}_1, \ddot{x}_2, \ddot{x}_3\}^T \tag{3.13}$$

2. $n_e = 6$, when both the translational and rotational acceleration components are considered.

$$\{E\} = \{\ddot{x}_1, \ddot{x}_2, \ddot{x}_3, \ddot{\theta}_1, \ddot{\theta}_2, \ddot{\theta}_3\}^T \tag{3.14}$$

3. $n_e = 9$, when the complete set with three translational acceleration, three rotational acceleration, and three rotational velocity excitation terms is considered.

$$\{E\} = \{\ddot{x}_1, \ddot{x}_2, \ddot{x}_3, \ddot{\theta}_1, \ddot{\theta}_2, \ddot{\theta}_3, \dot{\theta}_1, \dot{\theta}_2, \dot{\theta}_3\}^T \tag{3.15}$$

Substituting equation (3.12) into equation (3.11) produces an expression connecting the rotor modal response with the input motions at the base as:

$$S(t) = \sum_{j=1}^{2n_t} \{\eta\}_j^T \int_0^t e^{\lambda_j(t-\tau)} \{E(\tau)\} d\tau \tag{3.16}$$

where

$$\{\eta\}_j = \{T\}^T \{\psi_R\}_j [r]^T \{\psi_L\}_j$$

3.3 Random Vibration Formulations

In the response spectrum approach, the earthquake induced ground motion components at the base of the machines are modeled as correlated stationary random processes. For such excitations, we first obtain the root mean square response which is calculated for stochastic inputs characterized by their spectral density functions. This response value is then amplified by a peak factor to obtain the maximum response, or the design response, of the system. This design response can finally be expressed in terms of the spectra of the base motion components.

To define the correlation between the components of the base motion, here the travelling seismic wave model is used for machines sitting on the ground. In this model, the rotational components are expressed as the spatial derivatives of the translational components as originally proposed by Newmark (1969). For the machines located in a building, the corelation between the input components at the base of the machine is determined by the response analysis of the building. The auto and cross floor response spectra are then used to define the correlation matrix for the calculation of the design response of the rotating system. Both cases are considered in the following sections.

3.3.1 Travelling Seismic Wave Model

Earthquake motions felt by a structure with respect to an arbitrary set of axes are generally statistically correlated. One way to study the effect of this correlation is to model the ground motions as a travelling wave. It has been observed that a set of axes exist along which three ground motion components are uncorrelated. These orthogonal axes are called as the principal axes and the three corresponding

independent excitations are called as the principal exciation components. The input components acting along the axes of the structure can be expressed in terms of the principal components through certain transformations. The response of the structure will depend on the relative orientation of the structure with respect to the impinging wave. As this orientation will never be known in advance, it is of interest to obtain the maximum response irrespective of the structural orientation. This maximum response is also referred to as the worst-case response. To compute this maximum response for a rotating machine, we will adopt an approach similar to the one used by Ghafory-Ashtiany and Singh (1986) for stationary civil structures.

Let (x_1, x_2, x_3) represent the structural coordinate system and (x_1', x_2', x_3') be the principal coordinate system. There is a geometric transformation matrix relating these two system of axes as:

$$\begin{Bmatrix} x_1 \\ x_2 \\ x_3 \end{Bmatrix} = [D]^T \begin{Bmatrix} x_1' \\ x_2' \\ x_3' \end{Bmatrix}, \quad [D] = \begin{bmatrix} d_{11} & d_{12} & d_{13} \\ d_{21} & d_{22} & d_{23} \\ d_{31} & d_{32} & d_{33} \end{bmatrix} \tag{3.17}$$

where d_{mn} =the direction cosine of the mth principal axis with respect to the nth structural axis. The translational acceleration components $\ddot{x}_1$ $\ddot{x}_2$ and $\ddot{x}_3$ along the structural axes can be expressed in terms of the principal excitations $\ddot{x}'_1$ $\ddot{x}'_2$ and $\ddot{x}'_3$ using the matrix of direction cosines as:

$$\begin{Bmatrix} \ddot{x}_1 \\ \ddot{x}_2 \\ \ddot{x}_3 \end{Bmatrix} = [D]^T \{E'\} \tag{3.18}$$

where $\{E'\} = \{\ddot{x}'_1, \ddot{x}'_2, \ddot{x}'_3\}^T$ is a (3×1) vector of principal excitation components. To obtain the base rotational input components, Ghafory-Ashtiany and Singh (1986) followed the method described by Newmark (1969) with some simplifying assumptions.

A rotational component of excitation was defined as:

$$\ddot{\theta}_k = -\frac{1}{2c}\frac{d}{dt}(\ddot{x}_j - \ddot{x}_i) \tag{3.19}$$

where c is the apparent wave velocity and i j k are in 1 2 3 permutations denoting the axes. In this research, we will also adopt equation (3.19) to develop a methodical procedure for including the rotational effects in the calculation of the rotor response.

Consistent with equation (3.19), the rotational accelerations and velocities with respect to the structural axes can then be written as follows:

$$\begin{Bmatrix} \ddot{\theta}_1 \\ \ddot{\theta}_2 \\ \ddot{\theta}_3 \end{Bmatrix} = -\frac{1}{2c}\frac{d}{dt}\begin{bmatrix} 0 & -1 & 1 \\ 1 & 0 & -1 \\ -1 & 1 & 0 \end{bmatrix}\begin{Bmatrix} \ddot{x}_1 \\ \ddot{x}_2 \\ \ddot{x}_3 \end{Bmatrix} \tag{3.20}$$

$$= -\frac{1}{2c}\frac{d}{dt}\begin{bmatrix} 0 & -1 & 1 \\ 1 & 0 & -1 \\ -1 & 1 & 0 \end{bmatrix}[D]^T\{E'\} \tag{3.21}$$

and

$$\begin{Bmatrix} \dot{\theta}_1 \\ \dot{\theta}_2 \\ \dot{\theta}_3 \end{Bmatrix} = -\frac{1}{2c}\begin{bmatrix} 0 & -1 & 1 \\ 1 & 0 & -1 \\ -1 & 1 & 0 \end{bmatrix}\begin{Bmatrix} \ddot{x}_1 \\ \ddot{x}_2 \\ \ddot{x}_3 \end{Bmatrix} \tag{3.22}$$

$$= -\frac{1}{2c}\begin{bmatrix} 0 & -1 & 1 \\ 1 & 0 & -1 \\ -1 & 1 & 0 \end{bmatrix}[D]^T\{E'\} \tag{3.23}$$

By consolidating the above equations, we can write for the complete base motion inputs to the rotor in terms of the principal excitations as follows:

$$\{E(t)\} = ([G_1]^T + \frac{1}{2c}\frac{d}{dt}[G_2]^T)[D]^T\{E'(t)\} \tag{3.24}$$

in which the auxiliary transformation matrices $[G_1]$ and $[G_2]$ are different for each case of the excitation vector $\{E\}$. These are defined as follows:

1. For three-component input, $\{E\} = \{\ddot{x}_1, \ddot{x}_2, \ddot{x}_3\}^T$

$$
\begin{aligned}
[G_1] &= \begin{bmatrix} 1 & 0 & 0 \\ 0 & 1 & 0 \\ 0 & 0 & 1 \end{bmatrix}_{3\times 3} \\
[G_2] &= \begin{bmatrix} 0 & 0 & 0 \\ 0 & 0 & 0 \\ 0 & 0 & 0 \end{bmatrix}_{3\times 3}
\end{aligned}
\tag{3.25}
$$

2. For six-component input, $\{E\} = \{\ddot{x}_1, \ddot{x}_2, \ddot{x}_3, \ddot{\theta}_1, \ddot{\theta}_2, \ddot{\theta}_3\}^T$

$$
\begin{aligned}
[G_1] &= \begin{bmatrix} 1 & 0 & 0 & 0 & 0 & 0 \\ 0 & 1 & 0 & 0 & 0 & 0 \\ 0 & 0 & 1 & 0 & 0 & 0 \end{bmatrix}_{3\times 6} \\
[G_2] &= \begin{bmatrix} 0 & 0 & 0 & 0 & -1 & 1 \\ 0 & 0 & 0 & 1 & 0 & -1 \\ 0 & 0 & 0 & -1 & 1 & 0 \end{bmatrix}_{3\times 6}
\end{aligned}
\tag{3.26}
$$

3. For nine-component input, $\{E\} = \{\ddot{x}_1, \ddot{x}_2, \ddot{x}_3, \ddot{\theta}_1, \ddot{\theta}_2, \ddot{\theta}_3, \dot{\theta}_1, \dot{\theta}_2, \dot{\theta}_3\}^T$

$$
\begin{aligned}
[G_1] &= \begin{bmatrix} 1 & 0 & 0 & 0 & 0 & 0 & 0 & -1/2c & 1/2c \\ 0 & 1 & 0 & 0 & 0 & 0 & 1/2c & 0 & -1/2c \\ 0 & 0 & 1 & 0 & 0 & 0 & -1/2c & 1/2c & 0 \end{bmatrix}_{3\times 9} \\
[G_2] &= \begin{bmatrix} 0 & 0 & 0 & 0 & -1 & 1 & 0 & 0 & 0 \\ 0 & 0 & 0 & 1 & 0 & -1 & 0 & 0 & 0 \\ 0 & 0 & 0 & -1 & 1 & 0 & 0 & 0 & 0 \end{bmatrix}_{3\times 9}
\end{aligned}
\tag{3.27}
$$

In order to get the worst-case response of a rotor under stochastic loadings one has to first evaluate the mean square response. For this we obtain the autocorrelation function for the response quantity $S(t)$ using equation (3.16)as follows:

$$Ex[S(t_1)S(t_2)] = \sum_{j=1}^{2n_t}\sum_{k=1}^{2n_t}\int_0^{t_1}\int_0^{t_2}\{\eta\}_j^T Ex[\{E(\tau_1)\}\{E(\tau_2)\}^T]\{\eta\}_k \\ e^{\lambda_j(t_1-\tau_1)}e^{\lambda_k(t_2-\tau_2)}d\tau_1 d\tau_2 \tag{3.28}$$

where $Ex[\ ]$ stands for the expected value. $Ex[\{E(\tau_1)\}\{E(\tau_2)\}^T]$ in the equation above is the correlation matrix of the structural excitations. It can be expanded in the following form for the model given by equation (3.24):

$$Ex[\{E(\tau_1)\}\{E(\tau_2)\}^T] = ([G_1]^T + \frac{1}{2c}\frac{d}{d\tau_1}[G_2]^T)[D]^T Ex[\{E'(\tau_1)\}\{E'(\tau_2)\}^T] \\ [D]([G_1] + \frac{1}{2c}\frac{d}{d\tau_2}[G_2]) \tag{3.29}$$

where $Ex[\{E'(\tau_1)\}\{E'(\tau_2)\}^T]$ now denotes the correlation matrix for principal excitations. This correlation matrix is a diagonal matrix of size (3×3) because the three principal components are uncorrelated.

Although the earthquake motions are not stationary in nature, the assumption that the principal inputs are stationary random processes has been found useful in earlier studies. This assumption is now widely employed for developing response spectrum methods used in seismic analysis of structures. In this work also we make this assumption to develop a spectrum approach for rotating machines.

For stationary principal excitation components, the correlation matrix can be expressed in terms of the spectral density function matrix as follows:

$$Ex[\{E'(\tau_1)\}\{E'(\tau_2)\}^T] = \int_{-\infty}^{\infty}[\Phi_P]e^{i\omega(\tau_1-\tau_2)}d\omega \tag{3.30}$$

where $[\Phi_P] = diag(\hat{\Phi}_l)$ for $l = 1, 2, 3$ with $\hat{\Phi}_l(\omega)$ being the spectral density function of the lth principal excitation. Combining equation (3.29) and equation (3.30) we then

obtain

$$Ex[\{E(\tau_1)\}\{E(\tau_2)\}^T] = \int_{-\infty}^{\infty}([G_1]^T + \frac{1}{2c}\frac{d}{d\tau_1}[G_2]^T)[D]^T[\Phi_P][D] \\ ([G_1] + \frac{1}{2c}\frac{d}{d\tau_2}[G_2])e^{i\omega(\tau_1-\tau_2)}d\omega \tag{3.31}$$

By making use of the following identity:

$$[D]^T[\Phi_P][D] = \sum_{l=1}^{3}\{d\}_l\hat{\Phi}_l(\omega)\{d\}_l^T$$

in which $\{d\}_l^T$ is the lth row of the direction cosine matrix $[D]$, equation (3.31) yields

$$Ex[\{E(\tau_1)\}\{E(\tau_2)\}^T] = \sum_{l=1}^{3}\int_{-\infty}^{\infty}([G_1]^T + \frac{1}{2c}\frac{d}{d\tau_1}[G_2]^T)\{d\}_l\{d\}_l^T \\ ([G_1] + \frac{1}{2c}\frac{d}{d\tau_2}[G_2])\hat{\Phi}_l(\omega)e^{i\omega(\tau_1-\tau_2)}d\omega \tag{3.32}$$

Expanding the previous equation and taking the proper time derivatives, the correlation matrix of the excitations with respect to the rotor coordinates can be written as follows:

$$Ex[\{E(\tau_1)\}\{E(\tau_2)\}^T] = \sum_{l=1}^{3}\int_{-\infty}^{\infty}\hat{\Phi}_l(\omega)\langle[G_1]^T\{d\}_l\{d\}_l^T[G_1] \\ +\frac{\omega^2}{4c^2}[G_2]^T\{d\}_l\{d\}_l^T[G_2] + \frac{i\omega}{2c}([G_2]^T\{d\}_l\{d\}_l^T[G_1] \\ -[G_1]\{d\}_l\{d\}_l^T[G_2])\rangle e^{i\omega(\tau_1-\tau_2)}d\omega \tag{3.33}$$

From equation (3.33) it can be clearly recognized that the first two terms indicate the autocorrelation effects of the translational and rotational inputs, respectively, while the remaining part describes the associated cross correlation between the translational and rotational components.

By substituting the correlation matrix given by equation (3.33) into equation (3.28) the autocorrelation function of response $S(t)$ becomes:

$$Ex[S(t_1)S(t_2)] = \sum_{l=1}^{3}\sum_{j=1}^{2n_t}\sum_{k=1}^{2n_t}\int_{-\infty}^{\infty}\hat{\Phi}_l(\omega)\{\eta\}_j^T$$

$$\langle [G_1]^T\{d\}_l\{d\}_l^T[G_1] + \frac{\omega^2}{4c^2}[G_2]^T\{d\}_l\{d\}_l^T[G_2]$$
$$+\frac{i\omega}{2c}([G_2]^T\{d\}_l\{d\}_l^T[G_1] - [G_1]^T\{d\}_l\{d\}_l^T[G_2])\rangle\{\eta\}_k$$
$$\int_0^{t_1}\int_0^{t_2} e^{\lambda_j(t_1-\tau_1)}e^{\lambda_k(t_2-\tau_2)}e^{i\omega(\tau_1-\tau_2)}d\tau_1 d\tau_2 d\omega \qquad (3.34)$$

In the equation shown above, the part involving the double integral over τ_1 and τ_2 can be carried out seperately. For a stationary process with relatively large t_1 and t_2 the integral can be obtained as follows:

$$\lim_{t_1,t_2\to\infty}\int_0^{t_1}\int_0^{t_2} e^{\lambda_j(t_1-\tau_1)+\lambda_k(t_2-\tau_2)+i\omega(\tau_1-\tau_2)}d\tau_1 d\tau_2 = \frac{e^{i\omega(t_1-t_2)}}{(i\omega-\lambda_j)(-i\omega-\lambda_k)}$$

Equation (3.34) hence can be written as

$$\begin{aligned} Ex[S(t_1)S(t_2)] &= \sum_{l=1}^{3}\sum_{j=1}^{2n_t}\sum_{k=1}^{2n_t}\int_{-\infty}^{\infty}\hat{\Phi}_l(\omega)\frac{e^{i\omega(t_1-t_2)}}{(i\omega-\lambda_j)(-i\omega-\lambda_k)} \\ &\quad \langle\{\eta\}_j^T[G_1]^T\{d\}_l\{d\}_l^T[G_1]\{\eta\}_k \\ &\quad +\frac{\omega^2}{4c^2}\{\eta\}_j^T[G_2]^T\{d\}_l\{d\}_l^T[G_2]\{\eta\}_k \\ &\quad +\frac{i\omega}{2c}(\{\eta\}_j^T[G_2]^T\{d\}_l\{d\}_l^T[G_1]\{\eta\}_k \\ &\quad -\{\eta\}_j^T[G_1]^T\{d\}_l\{d\}_l^T[G_2]\{\eta\})k)\rangle d\omega \end{aligned} \qquad (3.35)$$

The stationary mean square value of the rotor response at any time t can be calculated by setting $t_1 = t_2 = t$ in the expression for the autocorrelation function to render:

$$\begin{aligned} Ex[S^2(t)] &= \sum_{l=1}^{3}\sum_{j=1}^{2n_t}\sum_{k=1}^{2n_t}\int_{-\infty}^{\infty}\frac{\hat{\Phi}_l(\omega)}{(i\omega-\lambda_j)(-i\omega-\lambda_k)} \\ &\quad \langle\{\rho_1\}_j^T\{d\}_l\{d\}_l^T\{\rho_1\}_k + \frac{\omega^2}{4c^2}\{\rho_2\}_j^T\{d\}_l\{d\}_l^T\{\rho_2\}_k \\ &\quad +\frac{i\omega}{2c}(\{\rho_2\}_j^T\{d\}_l\{d\}_l^T\{\rho_1\}_k - \{\rho_1\}_j^T\{d\}_l\{d\}_l^T\{\rho_2\}_k)\rangle d\omega \end{aligned} \qquad (3.36)$$

in which $\{\rho_1\}_j$ and $\{\rho_2\}_j$ are (3×1) vectors defined as:

$$\{\rho_1\}_j = [G_1]\{\eta\}_j$$

$$\{\rho_2\}_j = [G_2]\{\eta\}_j \qquad (3.37)$$

Equation (3.36) can be further modified by utilizing the transpose property of scalar quantities, such as $\{\rho_1\}_j^T\{d\}_l = \{d\}_l^T\{\rho_1\}_j$. The mean square response can then be presented in a condensed form by matrix notations as:

$$\begin{aligned} Ex[S^2(t)] &= \sum_{l=1}^{3}\{d\}^T([R_1]_l + [R_2]_l + [R_3]_l)\{d\}_l \\ &= \sum_{l=1}^{3}\{d\}_l^T[R]_l\{d\}_l \end{aligned} \tag{3.38}$$

$[R]_l$ appearing in the equation above is a (3×3) Hermitian matrix with typical elements expressed in terms of the entries of matrices $[R_1]_l, [R_2]_l$ and $[R_3]_l$. They are defined as:

$$R_{mnl} = R_{1_{mnl}} + R_{2_{mnl}} + R_{3_{mnl}} \qquad m,n,l = 1,2,3$$

$$R_{1_{mnl}} = \int_{-\infty}^{\infty}\hat{\Phi}_l(\omega)\sum_{j=1}^{2n_t}\sum_{k=1}^{2n_t}\frac{\rho_{1jm}\rho_{1kn}}{(i\omega-\lambda_j)(-i\omega-\lambda_k)}d\omega$$

$$R_{2_{mnl}} = \int_{-\infty}^{\infty}\frac{\omega^2}{4c^2}\hat{\Phi}_l(\omega)\sum_{j=1}^{2n_t}\sum_{k=1}^{2n_t}\frac{\rho_{2jm}\rho_{2kn}}{(i\omega-\lambda_j)(-i\omega-\lambda_k)}d\omega$$

$$R_{3_{mnl}} = \int_{-\infty}^{\infty}\frac{i\omega}{2c}\hat{\Phi}_l(\omega)\sum_{j=1}^{2n_t}\sum_{k=1}^{2n_t}\frac{\rho_{2jm}\rho_{1kn}-\rho_{1jm}\rho_{2kn}}{(i\omega-\lambda_j)(-i\omega-\lambda_k)}d\omega \tag{3.39}$$

where ρ_{1jm} and ρ_{2kn} are the mth and nth elements of vectors $\{\rho_1\}_j$ and $\{\rho_2\}_k$ respectively.

To calculate the response by a spectrum approach, the elements of the matrices in equation (3.38) have to be expressed in terms of the modal frequencies and damping ratios obtained from the eigenvalue analysis. It is necessary here to point out that in a rotating machine with fluid film bearings, there are usually some real eigenvalues and corresponding real eigenvectors in addition to the paired complex and conjugate eigenvalues and eigenvectors. These real eigenproperties require a somewhat different

treatment in the derivations. In the following formulation, the effect of the real eigenproperties on the response is seperated out from those of the complex eigenproperties. Let n_c be the number of real eigenvalues and n_r be the number of pairs of complex and conjugate ones, with $n_c + 2n_r = 2n_t$. We divide the real and complex eigenvalues λ_j and their corresponding modal coefficients ρ_{1jm} and ρ_{2jm} as follows:

- Real eigenproperties: for $j = 1$ to n_r,

$$\begin{cases} \lambda_j^r = -\alpha_j, \quad \alpha_j > 0 \\ \rho_{1jm}^r = e_{1jm} \\ \rho_{2jm}^r = e_{2jm} \end{cases} \tag{3.40}$$

- Complex eigenproperties: for $j = 1$ to n_c,

$$\begin{cases} \lambda_j^c = -\beta_j\omega_j + i\omega_j\sqrt{1-\beta_j^2} \\ \rho_{1jm}^c = a_{1jm} + ib_{1jm} \\ \rho_{2jm}^c = a_{2jm} + ib_{2jm} \end{cases} \tag{3.41}$$

- Complex conjugate eigenproperties: for $j = 1$ to n_c,

$$\begin{cases} \lambda_j^{cc} = -\beta_j\omega_j - i\omega_j\sqrt{1-\beta_j^2} \\ \rho_{1jm}^{cc} = a_{1jm} - ib_{1jm} \\ \rho_{2jm}^{cc} = a_{2jm} - ib_{2jm} \end{cases} \tag{3.42}$$

where the superscripts r, c, and cc denote real, complex, and complex conjugate.

The subsequent derivations are focused on $[R_1]_l$ alone and the formulations for $[R_2]_l$ and $[R_3]_l$ can be constructed in the same way. Consider a summation term over index j appearing in $R_{1_{mnl}}$ shown in equation (3.39). We split this summation term into its real and complex modes as follows:

$$\sum_{j=1}^{2n_t} \frac{\rho_{1jm}}{i\omega - \lambda_j} = \sum_{j=1}^{n_r} \frac{\rho_{1jm}^r}{i\omega - \lambda_j^r} + \sum_{j=1}^{n_c} \left(\frac{\rho_{1jm}^c}{i\omega - \lambda_j^c} + \frac{\rho_{1jm}^{cc}}{i\omega - \lambda_j^{cc}} \right)$$

$$= \sum_{j=1}^{n_r} \frac{e_{1jm}}{i\omega + \alpha_j} + 2\sum_{j=1}^{n_c}(z_{1jm} + i\omega a_{1jm})H_j(\omega) \tag{3.43}$$

where equations (3.40), (3.41) and (3.42) have been used to define terms in (3.43) as:

$$\begin{aligned} z_{1jm} &= a_{1jm}\beta_j\omega_j - b_{1jm}\omega_j\sqrt{1-\beta_j^2} \\ H_j &= \frac{1}{\omega_j^2 - \omega_2 + 2i\omega\beta_j\omega_j} \end{aligned} \tag{3.44}$$

Similarly, we can write for the other summation term over index k as:

$$\sum_{k=1}^{2n_t} \frac{\rho_{1kn}}{-i\omega - \lambda_k} = \sum_{k=1}^{n_r} \frac{e_{1kn}}{-i\omega + \alpha_k} + 2\sum_{k=1}^{n_c}(z_{1kn} - i\omega a_{1kn})H_k^*(\omega) \tag{3.45}$$

In these two expressions H_j is the classical frequency response function of a second order differential equation of a single degree of freedom oscillator with frequency ω_j and damping ratio β_j and the asterisk $(*)$ as superscript means complex conjugate. Substituting equations (3.43) and (3.45) into equation (3.39) provides:

$$R_{1_{mnl}} = \int_{-\infty}^{\infty} \hat{\Phi}_l(\omega)(\Gamma_{1_{mn}} + \Gamma_{2_{mn}} + \Gamma_{3_{mn}})d\omega \tag{3.46}$$

where

$$\begin{aligned} \Gamma_{1_{mn}} &= \sum_{j=1}^{n_r}\sum_{k=1}^{n_r}(\frac{e_{1jm}}{i\omega + \alpha_j})(\frac{e_{1kn}}{-i\omega + \alpha_k}) \\ \Gamma_{2_{mn}} &= 2\sum_{j=1}^{n_r}\sum_{k=1}^{n_c}(\frac{e_{1jm}}{i\omega + \alpha_j})(z_{1kn} - i\omega a_{1kn})H_k^* \\ &\quad +2\sum_{j=1}^{n_c}\sum_{k=1}^{n_r}(\frac{e_{1kn}}{-i\omega + \alpha_k})(z_{1jm} + i\omega a_{1jm})H_j \\ \Gamma_{3_{mn}} &= 4\sum_{j=1}^{n_c}\sum_{k=1}^{n_c}(z_{1jm} + i\omega a_{1jm})(z_{1kn} - i\omega a_{1kn})H_jH_k^* \end{aligned} \tag{3.47}$$

Through extensive algebraic manipulations $\Gamma_{1_{mn}}$, $\Gamma_{2_{mn}}$, and $\Gamma_{3_{mn}}$ can be reduced to the following more useful form:

$$\begin{aligned} \Gamma_{1_{mn}} &= \sum_{j=1}^{n_r}\frac{e_{1jm}e_{1jn}}{\omega^2 + \alpha_j^2} + \sum_{j=1}^{n_r-1}\sum_{k=j+1}^{n_r}(\frac{e_{1jm}e_{1kn} + e_{1jn}e_{1km}}{\alpha_j + \alpha_k})(\frac{\alpha_j}{\omega^2 + \alpha_j^2} + \frac{\alpha_k}{\omega^2 + \alpha_k^2}) \\ \Gamma_{2_{mn}} &= 2\sum_{j=1}^{n_c}\sum_{k=1}^{n_r}(L_0 + L_2\omega^2 + L_4\omega^4)\frac{|H_j|^2}{\omega^2 + \alpha_k^2} \end{aligned}$$

$$\Gamma_{3_{mn}} = 4\sum_{j=1}^{n_c}(z_{1jm}z_{1jn} + a_{1jm}a_{1jn}\omega^2)|H_j|^2 + 4\sum_{j=1}^{n_c-1}\sum_{k=j+1}^{n_c}(N_0 + N_2\omega^2 + N_4\omega^4 + N_6\omega^6)|H_j|^2|H_k|^2 \quad (3.48)$$

where (L_0,L_2,L_4) and (N_0,N_2,N_4,N_6) are all constants and the explicit expressions of these quantities which also are functions of indices j, k, m and n are listed in Appendix B. In order to present $R_{1_{mnl}}$ in terms of the frequency integrals which are associated with the input spectra required in the spectrum approach, terms in $\Gamma_{2_{mn}}$ and $\Gamma_{3_{mn}}$ need to be further expanded into partial fractions as:

$$(L_0 + L_2\omega^2 + L_4\omega^4)\frac{|H_j|^2}{\omega^2 + \alpha_k^2} = \frac{U}{\omega^2 + \alpha_k^2} + V|H_j|^2 + W\omega^2|H_j|^2$$

$$(N_0 + N_2\omega^2 + N_4\omega^4 + N_6\omega^6)|H_j|^2|H_k|^2 = X_j|H_j|^2 + Y_j\omega^2|H_j|^2 + X_k|H_k|^2 + Y_k\omega^2|H_k|^2 \quad (3.49)$$

in which (U,V,W) and (X_j,Y_j,X_k,Y_k) are defined as follows:

$$\begin{cases} W = [L_4(\omega_j^4 - \alpha_k^2 g_j) + L_2\alpha_k^2 - L_0]/(\alpha_k^4 + \omega_j^4 - \alpha_k^2 g_j) \\ V = [L_0 + \omega_j^4(W - L_4)]/\alpha_k^2 \\ U = L_4 - W \end{cases} \quad (3.50)$$

and

$$\begin{cases} X_k = \frac{1}{\Delta_{jk}}[(\omega_j^4 - \omega_k^4)(N_4 - g_k N_6 - \omega_k^{-4}N_0) - (g_j - g_k)(N_2 - \omega_k^4 N_6 - \omega_k^{-4}g_k N_0)] \\ Y_k = \frac{1}{\Delta_{jk}}[(1 - \Omega_{jk}^4)(N_2 - \omega_k^4 N_6 - \omega_k^{-4}g_k N_0) - (g_j - \Omega_{jk}^4 g_k)(N_4 - g_k N_6 - \omega_k^{-4}N_0)] \\ X_j = \frac{1}{\omega_k^4}(N_0 - \omega_j^4 X_k) \\ Y_j = N_6 - Y_k \end{cases} \quad (3.51)$$

where

$$
\begin{aligned}
g_j &= \omega_j^2(4\beta_j^2 - 2) \\
g_k &= \omega_k^2(4\beta_k^2 - 2) \\
\Omega_{jk} &= \frac{\omega_j}{\omega_k} \\
\Delta_{jk} &= (\omega_j^4 - \omega_k^4)(1 - \Omega_{jk}^4) - (g_j - g_k)(g_j - \Omega_{jk}^4 g_k)
\end{aligned}
$$

Based on equations (3.46), (3.48) and (3.49), the final form of $R_{1_{mnl}}$ is written as:

$$
\begin{aligned}
R_{1_{mnl}} &= \sum_{j=1}^{n_r} e_{1jm}e_{1jn}\hat{J}_{0lj} + \sum_{j=1}^{n_r-1}\sum_{k=j+1}^{n_r}\left(\frac{e_{1jm}e_{1kn} + e_{1jn}e_{1km}}{\alpha_j + \alpha_k}\right)(\alpha_j\hat{J}_{0lj} + \alpha_k\hat{J}_{0lk}) \\
&\quad +2\sum_{j=1}^{n_c}\sum_{k=1}^{n_r}(U_1\hat{J}_{0lk} + V_1\hat{I}_{0lj} + W_1\hat{I}_{2lj}) \\
&\quad +4\sum_{j=1}^{n_c}(z_{1jm}z_{1jn}\hat{I}_{0lj} + a_{1jm}a_{1jn}\hat{I}_{2lj}) \\
&\quad +4\sum_{j=1}^{n_c-1}\sum_{k=j+1}^{n_c}(X_{j1}\hat{I}_{0lj} + Y_{j1}\hat{I}_{2lj} + X_{k1}\hat{I}_{0lk} + Y_{k1}\hat{I}_{2lk})
\end{aligned} \tag{3.52}
$$

where

$$
\begin{aligned}
\hat{J}_{0lj} &= \int_{-\infty}^{\infty}\frac{\hat{\Phi}_l(\omega)}{\omega^2 + \alpha_j^2}d\omega \\
\hat{I}_{0lj} &= \int_{-\infty}^{\infty}|H_j|^2\hat{\Phi}_l(\omega)d\omega \\
\hat{I}_{2lj} &= \int_{-\infty}^{\infty}|H_j|^2\omega^2\hat{\Phi}_l(\omega)d\omega
\end{aligned} \tag{3.53}
$$

Note that the supplementary subscripts 1 for (U,V,W) and (X_j,Y_j,X_k,Y_k) appearing in equation (3.52) indicate that these computed coefficients correspond to the part $[R_1]_l$ to distinguish from those obtained for $[R_2]_l$ and $[R_3]_l$. It can be recognized from the expression for $R_{1_{mnl}}$ that the terms under single summation designate the contributions from the individual modes whereas those under double summation indicate the effect from the interaction between the modes, real as well as complex ones.

The frequency integrals $\hat{I}_{0lj}$ and $\hat{I}_{2lj}$ defined in equation (3.53) are the mean square values of the relative displacement and relative velocity responses, respectively, of an oscillator with dynamic parameters ω_j and β_j subjected to the principal excitation in the lth direction. Likewise, $\hat{J}_{0lj}$ represents the mean square response for the relative velocity of a massless oscillator with frquency α_j under the lth principal excitation. The governing differential equations of these two systems are:

$$\ddot{u} + 2\beta_j\omega_j\dot{u} + \omega_j^2 u = \ddot{x}'_l(t)$$

$$\dot{v} + \alpha_j v = \ddot{x}'_l(t) \tag{3.54}$$

where u and v are the displacement and velocity responses and $\ddot{x}'_l$ is the seismic motion along lth principal direction. If only the translational inputs are considered in the analysis then from equation (3.39), $R_{mnl} = R_{1_{mnl}}$. Equation (3.52) itself can, therefore, be used to obtain the response matrix $[R]_l$ because the modal coefficient vector $\{\rho_2\}_j$ involved in calculating $[R_2]_l$ and $[R_3]_l$ is equal to zero for this case, as shown in equation (3.25).

The preceding procedure can also be applied to derive the expressions for $[R_2]_l$ and $[R_3]_l$. These expressions in their final form are presented in the following without repeated elaboration:

$$\begin{aligned} R_{2_{mnl}} = \frac{1}{4c^2}\{ & \sum_{j=1}^{n_r} e_{2jm}e_{2jn}\hat{J}_{2lj} \\ & + \sum_{j=1}^{n_r-1}\sum_{k=j+1}^{n_r}\left(\frac{e_{2jm}e_{2kn} + e_{2jn}e_{2km}}{\alpha_j + \alpha_k}\right)(\alpha_j\hat{J}_{2lj} + \alpha_k\hat{J}_{2lk}) \\ & + 2\sum_{j=1}^{n_c}\sum_{k=1}^{n_r}(U_2\hat{J}_{2lk} + V_2\hat{I}_{2lj} + W_2\hat{I}_{4lj}) \\ & + 4\sum_{j=1}^{n_c}(z_{2jm}z_{2jn}\hat{I}_{2lj} + a_{2jm}a_{2jn}\hat{I}_{4lj}) \\ & + 4\sum_{j=1}^{n_c-1}\sum_{k=j+1}^{n_c}(X_{j2}\hat{I}_{2lj} + Y_{j2}\hat{I}_{4lj} + X_{k2}\hat{I}_{2lk} + Y_{k2}\hat{I}_{4lk})\} \end{aligned} \tag{3.55}$$

and

$$
\begin{aligned}
R_{3_{mnl}} = \frac{1}{2c}\{ & \sum_{j=1}^{n_r-1}\sum_{k=j+1}^{n_r}\left(\frac{e_{1jm}e_{2kn}+e_{1jn}e_{2km}}{\alpha_j+\alpha_k}-\frac{e_{1km}e_{2jn}+e_{1kn}e_{2jm}}{\alpha_j+\alpha_k}\right) \\
& (\alpha_j^2\hat{J}_{0lj}-\alpha_k^2\hat{J}_{0lk}) \\
& +2\sum_{j=1}^{n_c}\sum_{k=1}^{n_r}(U_3\hat{J}_{0lk}+V_3\hat{I}_{0lj}+W_3\hat{I}_{2lj}) \\
& +4\sum_{j=1}^{n_c}(a_{1jm}z_{2jn}+a_{1jn}z_{2jm}-z_{1jm}a_{2jn}-z_{1jn}a_{2jm})\hat{I}_{2lj} \\
& +4\sum_{j=1}^{n_c-1}\sum_{k=j+1}^{n_c}(X_{j3}\hat{I}_{0lj}+Y_{j3}\hat{I}_{2lj}+X_{k3}\hat{I}_{0lk}+Y_{k3}\hat{I}_{2lk})\}
\end{aligned}
\tag{3.56}
$$

where

$$
\hat{J}_{2lj}=\int_{-\infty}^{\infty}\frac{\omega^2}{\omega^2+\alpha_j^2}\hat{\Phi}_l(\omega)d\omega
$$

$$
\hat{I}_{4lj}=\int_{-\infty}^{\infty}|H_j|^2\omega^4\hat{\Phi}_l(\omega)d\omega \tag{3.57}
$$

Two additional frequency integrals $\hat{I}_{4lj}$ and $\hat{J}_{2lj}$ are introduced in the above equations. These are the mean square values of the relative acceleration response for a single-degree-of-freedom oscillator (ω_j, β_j) and a massless oscillator (α_j) respectively. However, they can be expressed in terms of the previously defined frequency integrals as follows:

$$
\hat{I}_{4lj}=\hat{I}_l-g_j\hat{I}_{2lj}-\omega_j^4\hat{I}_{0lj}
$$

$$
\hat{J}_{2lj}=\hat{I}_l-\alpha_j^2\hat{J}_{0lj} \tag{3.58}
$$

where

$$
\hat{I}_l=\int_{-\infty}^{\infty}\hat{\Phi}_l(\omega)d\omega
$$

The integral $\hat{I}_l$ is the area under the spectral density function. It represents the mean square value of the ground acceleration when subjected to the lth principal

excitation. The subscripted constants (U_i,V_i,W_i), and (X_{ji},Y_{ji},X_{ki},Y_{ki}) are calculated through the process of partial fraction expansions described in equations (3.49), (3.50) and (3.51) in which the coefficients of polynomials $L(\omega) = L_0 + L_2\omega^2 + L_4\omega^4$ and $N(\omega) = N_0 + N_2\omega^2 + N_4\omega^4 + N_6\omega^6$ are provided in Appendix B for $[R_1]_l$, $[R_2]_l$, and $[R_3]_l$ individually.

Through the foregoing approach, the 3×3 response matrix $[R]_l$ can finally be written in terms of the dynamic properties of the rotor system and random response characteristics of the excitation inputs as follows:

$$\begin{aligned} R_{mnl} &= \sum_{j=1}^{n_r}\{\frac{e_{2jm}e_{2jn}}{4c^2}\hat{I}_l + (e_{1jm}e_{1jn} - \frac{e_{2jm}e_{2jn}\alpha_j^2}{4c^2})\hat{J}_{0lj}\} \\ &+ \sum_{j=1}^{n_r-1}\sum_{k=j+1}^{n_r}\{\frac{e_{2jm}e_{2kn} + e_{2jn}e_{2km}}{4c^2}\hat{I}_l + \mu_1^{rr}\hat{J}_{0lj} + \mu_2^{rr}\hat{J}_{0lk}\} \\ &+ \sum_{j=1}^{n_c}\sum_{k=1}^{n_r}\{\mu^{cr}\hat{I}_l + \bar{U}\hat{J}_{0lk} + \bar{V}\hat{I}_{0lj} + \bar{W}\hat{I}_{2lj}\} \\ &+ \sum_{j=1}^{n_c}\{\frac{a_{2jm}a_{2jn}}{c^2}\hat{I}_l + \mu_1^{c}\hat{I}_{0lj} + \mu_2^{c}\hat{I}_{2lj}\} \\ &+ \sum_{j=1}^{n_c-1}\sum_{k=j+1}^{n_c}\{\mu^{cc}\hat{I}_l + \bar{X}_j\hat{I}_{0lj} + \bar{Y}_j\hat{I}_{2lj} + \bar{X}_k\hat{I}_{0lk} + \bar{Y}_k\hat{I}_{2lk}\} \end{aligned} \tag{3.59}$$

in which the expressions for coefficients (μ_1^{rr},μ_2^{rr},μ^{cr},μ_1^{c},μ_2^{c},μ^{cc}), ($\bar{U}$,$\bar{V}$,$\bar{W}$) and ($\bar{X}_j$, $\bar{Y}_j$,$\bar{X}_k$,$\bar{Y}_k$) are tabulated in Appendix B.

With R_{mnl} defined as above, equation (3.38) can be used to calculate the rotor response if $\{d\}_l$ the direction of the attacking seismic wave is known. Since the orientation of the principal excitations relative to the rotor axis is impossible to predict, our goal is to obtain the worst-case response, that is, the maximum value of the reponse quantity irrespective of the direction of the coming wave. The methodology proposed by Ghafory-Ashtiany and Singh (1986) is adopted in this work to evaluate this maximum response.

3.3.2 Correlation Matrix Model

The preceding formulation developed from a seismic wave model can be used for analyzing rotating machines that are directly excitated by the ground motions. For the rotor systems mounted on the higher floors of a building, or placed on raised pedestals (like turbines in power plants), the base excitations are defined by the motion of the supports. The components of the support motion can be correlated in this case, even when the input motions at the base of the supporting structures are uncorrelated.

For stochastic analysis, the input correlation can be defined in terms of the correlation matrix. In this model, the correlation matrix is directly expressed in terms of the auto and cross spectral density functions of the base motion components. These auto and cross spectral density functions depend upon the characteristics of the supporting structure as well as the motion at the base of the structure. To define these auto and cross spectral density functions, a dynamic analysis of the primary structure is required. Assuming that the interaction between rotating machines and the supporting structure can be ignored, the method developed by Singh and Burdisso (1987) can be used to provide these auto and cross spectral density functions of the base excitation components.

In this model, the matrix of input correlation $Ex[\{E(\tau_1)\}\{E(\tau_2)\}^T]$ in equation (3.28) can be expressed as follows:

$$Ex[\{E(\tau_1)\}\{E(\tau_2)\}^T] = \int_{-\infty}^{\infty} [\Phi_{EE}(\omega)] e^{i\omega(\tau_1-\tau_2)} d\omega \tag{3.60}$$

where the spectral density function matrix $[\Phi_{EE}]$ is of size $(n_e \times n_e)$. Substituting the above equation in equation (3.28) and making use of the procedure presented in the previous section to carry out the double integral over τ_1 and τ_2, the mean square

response for $S(t)$ can be written in the following form:

$$\begin{aligned} Ex[S^2(t)] &= \sum_{j=1}^{2n_t}\sum_{k=1}^{2n_t}\int_{-\infty}^{\infty}\frac{\{\eta\}_j^T[\Phi_{EE}]\{\eta\}_k}{(i\omega-\lambda_j)(-i\omega-\lambda_k)}d\omega \\ &= \sum_{m=1}^{n_e}\sum_{n=1}^{n_e}\sum_{j=1}^{2n_t}\sum_{k=1}^{2n_t}\int_{-\infty}^{\infty}\Phi_{mn}(\omega)(\frac{\eta_{jm}}{i\omega-\lambda_j})(\frac{\eta_{kn}}{-i\omega-\lambda_k})d\omega \end{aligned} \tag{3.61}$$

in which Φ_{mn} denotes the typical entry in matrix $[\Phi_{EE}]$ and η_{jm} is the mth element of vector $\{\eta\}_j$.

The diagonal terms, $\Phi_m(\omega)$, appearing in the correlation matrix $[\Phi_{EE}]$ are the auto spectral density functions for each individual excitation. The off-diagonal elements $\Phi_{mn}(\omega)$ represent the cross spectral density functions characterizing the correlation between the corresponding two input components. For a random process the auto spectral density function is always a real and even function. The cross spectral density function of any two random processes is a complex function consisting of the coincident and quadrature components. In terms of these components we can write a cross spectral density function in the following manner:

$$\begin{aligned} \Phi_{mn}(\omega) &= \Phi_{mn}^R(\omega) + i\Phi_{mn}^I(\omega) \\ \Phi_{nm}(\omega) &= \Phi_{mn}^*(\omega) \\ &= \Phi_{mn}^R(\omega) - i\Phi_{mn}^I(\omega) \qquad m \neq n \end{aligned} \tag{3.62}$$

where the superscript$(*)$ marks for complex conjugate. The coincident $\Phi_{mn}^R(\omega)$ are even functions, whereas the quadrature $\Phi_{mn}^I(\omega)$ are odd functions. In the subsequent derivations, we will also use the following relationship:

$$\begin{aligned} \Phi_{mn} + \Phi_{nm} &= 2\Phi_{mn}^R \\ \Phi_{mn} - \Phi_{nm} &= 2i\Phi_{mn}^I \end{aligned} \tag{3.63}$$

To develop the expressions for the mean square response of $S(t)$, the eigenvalues and participation coefficients are divided into the real, complex, and complex

conjugate parts as follows:

$$\begin{cases} \lambda_j^r &= -\alpha_j \quad j = 1 \text{ to } n_r \\ \eta_{jm}^r &= e'_{jm} \end{cases}$$

$$\begin{cases} \lambda_j^c &= -\beta_j\omega_j + i\omega_j\sqrt{1-\beta_j^2} \quad j = 1 \text{ to } n_c \\ \eta_{jm}^c &= a'_{jm} + ib'_{jm} \end{cases}$$

$$\begin{cases} \lambda_j^{cc} &= -\beta_j\omega_j - i\omega_j\sqrt{1-\beta_j^2} \quad j = 1 \text{ to } n_c \\ \eta_{jm}^{cc} &= a'_{jm} - ib'_{jm} \end{cases} \tag{3.64}$$

Following the procedure presented in the previous section for the development of equations (3.43) and (3.45), the double summation term over indices j and k in equation (3.61) can also be rewritten in the following form:

$$\sum_{j=1}^{2n_t}\sum_{k=1}^{2n_t}\left(\frac{\eta_{jm}}{i\omega-\lambda_j}\right)\left(\frac{\eta_{kn}}{-i\omega-\lambda_k}\right) = \bar{\Gamma}_{1_{mn}} + \bar{\Gamma}_{2_{mn}} + \bar{\Gamma}_{3_{mn}} \tag{3.65}$$

where

$$\begin{aligned} \bar{\Gamma}_{1_{mn}} &= \sum_{j=1}^{n_r}\sum_{k=1}^{n_r}\left(\frac{e'_{jm}}{i\omega+\alpha_j}\right)\left(\frac{e'_{kn}}{-i\omega+\alpha_k}\right) \\ \bar{\Gamma}_{2_{mn}} &= 2\{\sum_{j=1}^{n_r}\sum_{k=1}^{n_c}\left(\frac{e'_{jm}}{i\omega+\alpha_j}\right)(z'_{kn} - i\omega a'_{kn})H_k^*(\omega) \\ &\quad + \sum_{j=1}^{n_c}\sum_{k=1}^{n_r}\left(\frac{e'_{kn}}{-i\omega+\alpha_k}\right)(z'_{jm} + i\omega a'_{jm})H_j(\omega)\} \\ \bar{\Gamma}_{3_{mn}} &= 4\sum_{j=1}^{n_c}\sum_{k=1}^{n_c}(z'_{jm} + i\omega a'_{jm})(z'_{kn} - i\omega a'_{kn})H_j(\omega)H_k^*(\omega) \end{aligned} \tag{3.66}$$

where

$$\begin{aligned} z'_{jm} &= a'_{jm}\beta_j\omega_j - b'_{jm}\omega_j\sqrt{1-\beta_j^2} \\ H_j &= \{(\omega_j^2 - \omega^2) + 2i\omega\beta_j\omega_j\}^{-1} \end{aligned}$$

The expression for the mean square response is also expanded as follows:

$$Ex[S^2(t)] = \sum_{m=1}^{n_e}\int_{-\infty}^{\infty}\Phi_{mm}(\bar{\Gamma}_{1_{mm}} + \bar{\Gamma}_{2_{mm}} + \bar{\Gamma}_{3_{mm}})d\omega$$

$$+\sum_{m=1}^{n_e-1}\sum_{n=m+1}^{n_e}\int_{-\infty}^{\infty}\{\Phi_{mn}(\bar{\Gamma}_{1_{mn}}+\bar{\Gamma}_{2_{mn}}+\bar{\Gamma}_{3_{mn}}) +\Phi_{nm}(\bar{\Gamma}_{1_{nm}}+\bar{\Gamma}_{2_{nm}}+\bar{\Gamma}_{3_{nm}})\}d\omega \tag{3.67}$$

in which each term has to be evaluated individually. The resulting forms are presented, without listing the details of the lengthy algebraic operations in the intermediate steps, as follows:

$$\bar{\Gamma}_{1_{mm}}\Phi_{mm} = \Phi_{mm}\{\sum_{j=1}^{n_r}\frac{{e'_{jm}}^2}{\omega^2+\alpha_j^2}+2\sum_{j=1}^{n_r-1}\sum_{k=j+1}^{n_r}\gamma_{mm}(\frac{\alpha_j}{\omega^2+\alpha_j^2}+\frac{\alpha_k}{\omega^2+\alpha_k^2})\}$$

$$\bar{\Gamma}_{2_{mm}}\Phi_{mm} = \Phi_{mm}\{2\sum_{j=1}^{n_c}\sum_{k=1}^{n_r}\frac{|H_j|^2}{\omega^2+\alpha_k^2}(L'_{10}+L'_{12}\omega^2+L'_{14}\omega^4)\}$$

$$\begin{aligned}\bar{\Gamma}_{3_{mm}}\Phi_{mm} = \Phi_{mm}\{&4\sum_{j=1}^{n_c}({z'_{jm}}^2+{a'_{jm}}^2\omega^2)|H_j|^2\\ &+4\sum_{j=1}^{n_c-1}\sum_{k=j+1}^{n_c}|H_j|^2|H_k|^2(N'_{10}+N'_{12}\omega^2+N'_{14}\omega^4+N'_{16}\omega^6)\}\end{aligned}$$

$$\begin{aligned}\bar{\Gamma}_{1_{mn}}\Phi_{mn}+\bar{\Gamma}_{1_{nm}}\Phi_{nm} = &(\Phi_{mn}+\Phi_{nm})\{\sum_{j=1}^{n_r}\frac{e'_{jm}e'_{jn}}{\omega^2+\alpha_j^2}\\ &+\sum_{j=1}^{n_r-1}\sum_{k=j+1}^{n_r}(\gamma_{mn}+\gamma_{nm})(\frac{\alpha_j}{\omega^2+\alpha_j^2}+\frac{\alpha_k}{\omega^2+\alpha_k^2})\}\\ &-(\Phi_{mn}-\Phi_{nm})\{\sum_{j=1}^{n_r-1}\sum_{k=j+1}^{n_r}i\omega(\gamma_{mn}-\gamma_{nm})\\ &(\frac{1}{\omega^2+\alpha_j^2}-\frac{1}{\omega^2+\alpha_k^2})\}\end{aligned}$$

$$\begin{aligned}\bar{\Gamma}_{2_{mn}}\Phi_{mn}+\bar{\Gamma}_{2_{nm}}\Phi_{nm} = &(\Phi_{mn}+\Phi_{nm})\{2\sum_{j=1}^{n_c}\sum_{k=1}^{n_r}\frac{|H_j|^2}{\omega^2+\alpha_k^2}\\ &(L'_{20}+L'_{22}\omega^2+L'_{24}\omega^4)\}\\ &-(\Phi_{mn}-\Phi_{nm})\{2\sum_{j=1}^{n_c}\sum_{k=1}^{n_r}i\omega\frac{|H_j|^2}{\omega^2+\alpha_k^2}\\ &(L'_{30}+L'_{32}\omega^2+L'_{34}\omega^4)\}\end{aligned}$$

$$\bar{\Gamma}_{3_{mn}}\Phi_{mn}+\bar{\Gamma}_{3_{nm}}\Phi_{nm} = (\Phi_{mn}+\Phi_{nm})\{4\sum_{j=1}^{n_c}(z'_{jm}z'_{jn}+a'_{jm}a'_{jn}\omega^2)|H_j|^2$$

$$
\begin{aligned}
&+4\sum_{j=1}^{n_c-1}\sum_{k=j+1}^{n_c}|H_j|^2|H_k|^2 \\
&(N'_{20}+N'_{22}\omega^2+N'_{24}\omega^4+N'_{26}\omega^6)\} \\
&-(\Phi_{mn}-\Phi_{nm})\{4\sum_{j=1}^{n_c} i\omega(a'_{jm}z'_{jn}-a'_{jn}z'_{jm})|H_j|^2 \\
&+4\sum_{j=1}^{n_c-1}\sum_{k=J=1}^{n_c} i\omega|H_j|^2|H_k|^2 \\
&(N'_{30}+N'_{32}\omega^2+N'_{34}\omega^4+N'_{36}\omega^6)\} \qquad (3.68)
\end{aligned}
$$

in which the constant γ_{mn} and the coefficients in polynomials $L'_i(\omega) = L'_{i0} + L'_{i2}\omega^2 + L'_{i4}\omega^4$ and $N'_i(\omega) = N'_{i0} + N'_{i2}\omega^2 + N'_{i4}\omega^4 + N'_{i6}\omega^6$, $i = 1, 2, 3$ are provided in Appendix C. These expressions can be further simplified by using the definitions for coincident and quadrature spectral functions given in equation (3.63). With the expansion of the terms into partial fractions, similar to those shown in equation (3.49), we obtain:

$$
\bar{\Gamma}_{1mm}\Phi_{mm} = \Phi_m\{\sum_{j=1}^{n_r}\frac{{e'_{jm}}^2}{\omega^2+\alpha_j^2}+2\sum_{j=1}^{n_r-1}\sum_{k=j+1}^{n_r}\gamma_{mm}(\frac{\alpha_j}{\omega^2+\alpha_j^2}+\frac{\alpha_k}{\omega^2+\alpha_k^2})\} \qquad (3.69)
$$

$$
\bar{\Gamma}_{2mm}\Phi_{mm} = \Phi_m\{2\sum_{j=1}^{n_c}\sum_{k=1}^{n_r}(\frac{U'_1}{\omega^2+\alpha_k^2}+V'_1|H_j|^2+W'_1\omega^2|H_j|^2)\} \qquad (3.70)
$$

$$
\begin{aligned}
\bar{\Gamma}_{3mm}\Phi_{mm} = \Phi_m\{&4\sum_{j=1}^{n_c}({z'_{jm}}^2|H_j|^2+{a'_{jm}}^2\omega^2|H_j|^2) \\
&+4\sum_{j=1}^{n_c-1}\sum_{k=j+1}^{n_c}(X'_{j1}|H_j|^2+Y'_{j1}\omega^2|H_j|^2 \\
&+X'_{k1}|H_k|^2+Y'_{k1}\omega^2|H_k|^2)\}
\end{aligned} \qquad (3.71)
$$

$$
\begin{aligned}
\bar{\Gamma}_{1mn}\Phi_{mn}+\bar{\Gamma}_{1nm}\Phi_{nm} = \Phi^R_{mn}\{&2\sum_{j=1}^{n_r}\frac{e'_{jm}e'_{jn}}{\omega^2+\alpha_j^2}+2\sum_{j=1}^{n_r-1}\sum_{k=j+1}^{n_r}(\gamma_{mn}+\gamma_{nm}) \\
&(\frac{\alpha_j}{\omega^2+\alpha_j^2}+\frac{\alpha_k}{\omega^2+\alpha_k^2})\} \\
&+\omega\Phi^I_{mn}\{2\sum_{j=1}^{n_r-1}\sum_{k=j+1}^{n_r}(\gamma_{mn}-\gamma_{nm}) \\
&(\frac{1}{\omega^2+\alpha_j^2}-\frac{1}{\omega^2+\alpha_k^2})\}
\end{aligned} \qquad (3.72)
$$

$$\begin{aligned}
\bar{\Gamma}_{2mn}\Phi_{mn} + \bar{\Gamma}_{2nm}\Phi_{nm} &= \Phi^R_{mn}\{4\sum_{j=1}^{n_c}\sum_{k=1}^{n_r}(\frac{U'_2}{\omega^2+\alpha_k^2} + V'_2|H_j|^2 + W'_2\omega^2|H_j|^2)\} \\
&\quad +\omega\Phi^I_{mn}\{4\sum_{j=1}^{n_c}\sum_{k=1}^{n_r}(\frac{U'_3}{\omega^2+\alpha_k^2} + V'_3|H_j|^2 \\
&\quad +W'_3\omega^2|H_j|^2)\} \qquad (3.73)
\end{aligned}$$

$$\begin{aligned}
\bar{\Gamma}_{3mn}\Phi_{mn} + \bar{\Gamma}_{3nm}\Phi_{nm} &= \Phi^R_{mn}\{8\sum_{j=1}^{n_c}(z'_{jm}z'_{jn}|H_j|^2 + a'_{jm}a'_{jn}\omega^2|H_j|^2) \\
&\quad +8\sum_{j=1}^{n_c-1}\sum_{k=j+1}^{n_c}(X'_{j2}|H_j|^2 + Y'_{j2}\omega^2|H_j|^2 \\
&\quad +X'_{k2}|H_k|^2 + Y'_{k2}\omega^2|H_k|^2)\} \\
&\quad +\omega\Phi^I_{mn}\{8\sum_{j=1}^{n_c}(a'_{jn}z'_{jm} - a'_{jm}z'_{jn})|H_j|^2 \\
&\quad +8\sum_{j=1}^{n_c-1}\sum_{k=j+1}^{n_c}(X'_{j3}|H_j|^2 + Y'_{j3}\omega^2|H_j|^2 \\
&\quad +X'_{k3}|H_k|^2 + Y'_{k3}\omega^2|H_k|^2)\} \qquad (3.74)
\end{aligned}$$

The response in equation (3.67) can be expressed through the six terms in equations (3.69) to (3.74). The first three terms represent the effect of individual excitation components, whereas the remaining three indicate the effect of their correlation with each other.

The mean square response shown in equation (3.67) can now be expressed in terms of the following frequency integrals defined for the auto, coincident, and quadrature power spectral density functions:

$$\begin{aligned}
I^A_{0jm} &= \int_{-\infty}^{\infty}|H_j|^2\Phi_m(\omega)d\omega \\
I^A_{2jm} &= \int_{-\infty}^{\infty}|H_j|^2\omega^2\Phi_m(\omega)d\omega \\
I^C_{0jmn} &= \int_{-\infty}^{\infty}|H_j|^2\Phi^R_{mn}(\omega)d\omega \\
I^C_{2jmn} &= \int_{-\infty}^{\infty}|H_j|^2\omega^2\Phi^R_{mn}(\omega)d\omega \\
I^Q_{0jmn} &= \int_{-\infty}^{\infty}|H_j|^2\omega\Phi^I_{mn}(\omega)d\omega \\
I^Q_{2jmn} &= \int_{-\infty}^{\infty}|H_j|^2\omega^3\Phi^I_{mn}(\omega)d\omega \qquad (3.75)
\end{aligned}$$

which are the mean square relative displacement and velocity responses of an oscillator with parameters ω_j and β_j, and

$$\begin{aligned} J^A_{jm} &= \int_{-\infty}^{\infty} \frac{1}{\omega^2+\alpha_j^2}\Phi_m(\omega)d\omega \\ J^C_{jmn} &= \int_{-\infty}^{\infty} \frac{1}{\omega^2+\alpha_j^2}\Phi^R_{mn}(\omega)d\omega \\ J^Q_{jmn} &= \int_{-\infty}^{\infty} \frac{\omega}{\omega^2+\alpha_j^2}\Phi^I_{mn}(\omega)d\omega \end{aligned} \tag{3.76}$$

equivalent to the mean square values for the relative velocity response of a massless oscillator with frequency α_j, under the random floor excitation characterized by the corresponding spectral functions. The final expression for the mean square response of a rotating machine can then be written in terms of the frequency integrals as follows:

$$\begin{aligned} Ex[S^2(t)] = & \sum_{m=1}^{n_e}\{\sum_{j=1}^{n_r} {e'_{jm}}^2 J^A_{jm} + \sum_{j=1}^{n_r-1}\sum_{k=j+1}^{n_r} 2\gamma_{mm}(\alpha_j J^A_{jm} + \alpha_k J^A_{km}) \\ & + \sum_{j=1}^{n_c}\sum_{k=1}^{n_r} 2(U'_1 J^A_{km} + V'_1 I^A_{0jm} + W'_1 I^A_{2jm}) \\ & + \sum_{j=1}^{n_c} 4({z'_{jm}}^2 I^A_{0jm} + {a'_{jm}}^2 I^A_{2jm}) \\ & + \sum_{j=1}^{n_c-1}\sum_{k=j+1}^{n_c} 4(X'_{j1} I^A_{0jm} + Y'_{j1} I^A_{2jm} + X'_{k1} I^A_{0km} + Y'_{k1} I^A_{2km})\} \\ & + \sum_{m=1}^{n_e-1}\sum_{n=m+1}^{n_e}\{\sum_{j=1}^{n_r} 2e'_{jm}e'_{jn} J^C_{jmn} \\ & + \sum_{j=1}^{n_r-1}\sum_{k=j+1}^{n_r}[2(\gamma_{mn}+\gamma_{nm})(\alpha_j J^C_{jmn} + \alpha_k J^C_{kmn}) \\ & +2(\gamma_{mn}-\gamma_{nm})(J^Q_{jmn} - J^Q_{kmn})] \\ & + \sum_{j=1}^{n_c}\sum_{k=1}^{n_r}[4(U'_2 J^C_{kmn} + V'_2 I^C_{0jmn} + W'_2 I^C_{2jmn}) \\ & +4(U'_3 J^Q_{kmn} + V'_3 I^Q_{0jmn} + W'_3 I^Q_{2jmn})] \\ & + \sum_{j=1}^{n_c} 8[z'_{jm}z'_{jn} I^C_{0jmn} + a'_{jm}a'_{jn} I^C_{2jmn} \\ & +(a'_{jn}z'_{jm} - a'_{jm}z'_{jn}) I^Q_{0jmn}] \\ & + \sum_{j=1}^{n_c-1}\sum_{k=j+1}^{n_c}[8(X'_{j2} I^C_{0jmn} + Y'_{j2} I^C_{2jmn} + X'_{k2} I^C_{0kmn} + Y'_{k2} I^C_{2kmn}) \end{aligned}$$

$$+8(X'_{j3}I^{Q}_{0jmn} + Y'_{j3}I^{Q}_{2jmn} + X'_{k3}I^{Q}_{0kmn} + Y'_{k3}I^{Q}_{2kmn})]\} \quad (3.77)$$

3.4 Response Spectrum Approach

The formulation derived in the previous sections provides a step-by step methodology for obtaining the root mean square response of a rotor system. For design purposes, however, the maximum response or the design response is of primary interest. Here we will extend equation (3.59) and (3.77) to obtain the design response of a rotating machine by a response spectrum approach where the base inputs defined in terms of ground response spectra or floor response spectra can be directly used.

To calculate the design response S_d, the root mean square value should be amplified by an appropriate peak factor as:

$$S_d = P_s\sqrt{Ex[S^2(t)]} \quad (3.78)$$

where P_s is the corresponding peak factor which is usually related to the level of probability of exceedance. In order to obtain the design response in equation (3.78) the frequency integrals involving spectral density functions will have to be expressed in terms of response spectrum values, since in the response spectrum method the base motions are described by the response spectra curves.

Let $\mathcal{P}_{lj}$ and $\mathcal{V}_{lj}$ represent, respectively, the pseudo acceleration and relative velocity ground response spectra of the lth input component at frequency ω_j and damping ratio β_j, and $\mathcal{G}_l$ represent the lth maximum ground acceleration; likewise, the relative velocity response spectrum for a massless oscillator with parameter α_j subjected to the lth excitation is denoted by $\mathcal{Z}_{lj}$. Then, the frequency integrals can also be written

in terms of the above response spectrum quantities as follows:

$$\begin{aligned}
\hat{I}_l &= (\frac{\mathcal{G}_l}{P_{g_l}})^2 \\
\hat{I}_{0lj} &= (\frac{\mathcal{P}_{lj}}{P_{a_{lj}}\omega_j^2})^2 \\
\hat{I}_{2lj} &= (\frac{\mathcal{V}_{lj}}{P_{v_{lj}}})^2 \\
\hat{J}_{0lj} &= (\frac{\mathcal{Z}_{lj}}{P_{z_{lj}}})^2
\end{aligned} \tag{3.79}$$

where P_{g_l}, $P_{a_{lj}}$, $P_{v_{lj}}$, and $P_{z_{lj}}$ are the associated peak factors. From equations (3.78) and (3.79) the squared maximum response of the rotor based on the seismic wave model is expressed as:

$$\begin{aligned}
{S_d}^2 &= P_s^2 \sum_{l=1}^{3} \{d\}_l^T [R]_l \{d\}_l \\
&= \sum_{l=1}^{3} \{d\}_l^T [\mathcal{R}]_l \{d\}_l
\end{aligned} \tag{3.80}$$

where $[\mathcal{R}]_l = P_s^2 [R]_l$ is the response matrix of input ground spectra. Each term of $[\mathcal{R}]_l$ is obtained through multiplying the corresponding element in $[R]_l$ by the response design peak factor P_s^2, which renders the following expression:

$$\begin{aligned}
\mathcal{R}_{mnl} &= \sum_{j=1}^{n_r} \{\frac{e_{2jm}e_{2jn}}{4c^2}\mathcal{G}_l^2 Q_{g_l}^2 + (e_{1jm}e_{1jn} - \frac{e_{2jm}e_{2jn}\alpha_j^2}{4c^2})\mathcal{Z}_{lj}^2 Q_{z_{lj}}^2\} \\
&\quad + \sum_{j=1}^{n_r-1}\sum_{k=j+1}^{n_r} \{\frac{e_{2jm}e_{2kn}+e_{2jn}e_{2km}}{4c^2}\mathcal{G}_l^2 Q_{g_l}^2 + \mu_1^{rr}\mathcal{Z}_{lj}^2 Q_{z_{lj}}^2 + \mu_2^{rr}\mathcal{Z}_{lk}^2 Q_{z_{lk}}^2\} \\
&\quad + \sum_{j=1}^{n_c}\sum_{k=1}^{n_r} \{\mu^{cr}\mathcal{G}_l^2 Q_{g_l}^2 + \bar{U}\mathcal{Z}_{lk}^2 Q_{z_{lk}}^2 + \bar{V}\frac{\mathcal{P}_{lj}^2}{\omega_j^4} Q_{a_{lj}}^2 + \bar{W}\mathcal{V}_{lj}^2 Q_{v_{lj}}^2\} \\
&\quad + \sum_{j=1}^{n_c} \{\frac{a_{2jm}a_{2jn}}{c^2}\mathcal{G}_l^2 Q_{g_l}^2 + \mu_1^c \frac{\mathcal{P}_{lj}^2}{\omega_j^4} Q_{a_{lj}}^2 + \mu_2^c \mathcal{V}_{lj}^2 Q_{v_{lj}}^2\} \\
&\quad + \sum_{j=1}^{n_c-1}\sum_{k=j+1}^{n_c} \{\mu^{cc}\mathcal{G}_l^2 Q_{g_l}^2 + \bar{X}_j \frac{\mathcal{P}_{lj}^2}{\omega_j^4} Q_{a_{lj}}^2 + \bar{Y}_j \mathcal{V}_{lj}^2 Q_{v_{lj}}^2 \\
&\qquad + \bar{X}_k \frac{\mathcal{P}_{lk}^2}{\omega_k^4} Q_{a_{lk}}^2 + \bar{Y}_k \mathcal{V}_{lk}^2 Q_{v_{lk}}^2\}
\end{aligned} \tag{3.81}$$

in which Q_{g_l}, $Q_{a_{lj}}$, $Q_{v_{lj}}$, and $Q_{z_{lj}}$ are the peak factor ratios defined as:

$$Q_{g_l} = \frac{P_s}{P_{g_l}}$$

$$
\begin{aligned}
Q_{a_{lj}} &= \frac{P_s}{P_{a_{lj}}} \\
Q_{v_{lj}} &= \frac{P_s}{P_{v_{lj}}} \\
Q_{z_{lj}} &= \frac{P_s}{P_{z_{lj}}}
\end{aligned} \tag{3.82}
$$

In equation (3.81) every term is associated with a peak factor ratio. These peak factor ratios can be different from one another and they can be analytically determined if desired. Nevertheless, often such refinements may not be necessary. It is commonly assumed that the modal peak factors for the base acceleration and for the pseudo acceleration and relative velocity responses of a single degree of freedom system as well as for a massless oscillator are the same as P_s. This implies that all ratios in equation (3.82) are equal to one. Under this assumption, equation (3.81) is simplified to provide the following expression for calculating the design response in terms of the base motion spectra:

$$
\begin{aligned}
\mathcal{R}_{mnl} = & \sum_{j=1}^{n_r} \{ \frac{e_{2jm} e_{2jn}}{4c^2} \mathcal{G}_l^2 + (e_{1jm} e_{1jn} - \frac{e_{2jm} e_{2jn} \alpha_j^2}{4c^2}) \mathcal{Z}_{lj}^2 \} \\
& + \sum_{j=1}^{n_r-1} \sum_{k=j+1}^{n_r} \{ \frac{e_{2jm} e_{2kn} + e_{2jn} e_{2km}}{4c^2} \mathcal{G}_l^2 + \mu_1^{rr} \mathcal{Z}_{lj}^2 + \mu_2^{rr} \mathcal{Z}_{lk}^2 \} \\
& + \sum_{j=1}^{n_c} \sum_{k=1}^{n_r} \{ \mu^{cr} \mathcal{G}_l^2 + \bar{U} \mathcal{Z}_{lk}^2 + \bar{V} \frac{\mathcal{P}_{lj}^2}{\omega_j^4} + \bar{W} \mathcal{V}_{lj}^2 \} \\
& + \sum_{j=1}^{n_c} \{ \frac{a_{2jm} a_{2jn}}{c^2} \mathcal{G}_l^2 + \mu_1^c \frac{\mathcal{P}_{lj}^2}{\omega_j^4} + \mu_2^c \mathcal{V}_{lj}^2 \} \\
& + \sum_{j=1}^{n_c-1} \sum_{k=j+1}^{n_c} \{ \mu^{cc} \mathcal{G}_l^2 + \bar{X}_j \frac{\mathcal{P}_{lj}^2}{\omega_j^4} + \bar{Y}_j \mathcal{V}_{lj}^2 + \bar{X}_k \frac{\mathcal{P}_{lk}^2}{\omega_k^4} + \bar{Y}_k \mathcal{V}_{lk}^2 \}
\end{aligned} \tag{3.83}
$$

By comparing this equation with equation (3.59), it is evident that the design response can be directly computed from equation (3.59) if all the frequency integrals appearing in that expression are replaced by the corresponding input spectrum values. Making the similar assumption about the equality of the peak factors in the expressions derived for the correlation matrix model, we can also develop a spectrum

approach for calculating the design response for this case as follows:

$$
\begin{aligned}
Ex[S^2(t)] \;=\; & \sum_{m=1}^{n_e}\{\sum_{j=1}^{n_r} {e'_{jm}}^2(\mathcal{Z}^A_{jm})^2 + \sum_{j=1}^{n_r-1}\sum_{k=j+1}^{n_r} 2\gamma_{mm}[\alpha_j(\mathcal{Z}^A_{jm})^2 + \alpha_k(\mathcal{Z}^A_{km})^2] \\
& + \sum_{j=1}^{n_c}\sum_{k=1}^{n_r} 2[U'_1(\mathcal{Z}^A_{km})^2 + V'_1(\frac{\mathcal{P}^A_{jm}}{\omega_j^2})^2 + W'_1(\mathcal{V}^A_{jm})^2] \\
& + \sum_{j=1}^{n_c} 4[{z'_{jm}}^2(\frac{\mathcal{P}^A_{jm}}{\omega_j^2})^2 + {a'_{jm}}^2(\mathcal{V}^A_{jm})^2] \\
& + \sum_{j=1}^{n_c-1}\sum_{k=j+1}^{n_c} 4[X'_{j1}(\frac{\mathcal{P}^A_{jm}}{\omega_j^2})^2 + Y'_{j1}(\mathcal{V}^A_{jm})^2 \\
& \quad + X'_{k1}(\frac{\mathcal{P}^A_{km}}{\omega_k^2})^2 + Y'_{k1}(\mathcal{V}^A_{km})^2]\} \\
& + \sum_{m=1}^{n_e-1}\sum_{n=m+1}^{n_e}\{\sum_{j=1}^{n_r} 2e'_{jm}e'_{jn}(\mathcal{Z}^C_{jmn})^2 \\
& \quad + \sum_{j=1}^{n_r-1}\sum_{k=j+1}^{n_r}\langle 2(\gamma_{mn}+\gamma_{nm})[\alpha_j(\mathcal{Z}^C_{jmn})^2 + \alpha_k(\mathcal{Z}^C_{kmn})^2] \\
& \quad + 2(\gamma_{mn}-\gamma_{nm})[(\mathcal{Z}^Q_{jmn})^2 - (\mathcal{Z}^Q_{kmn})^2]\rangle \\
& \quad + \sum_{j=1}^{n_c}\sum_{k=1}^{n_r}\langle 4[U'_2(\mathcal{Z}^C_{kmn})^2 + V'_2(\frac{\mathcal{P}^C_{jmn}}{\omega_j^2})^2 + W'_2(\mathcal{V}^C_{jmn})^2] \\
& \quad + 4[U'_3(\mathcal{Z}^Q_{kmn})^2 + V'_3(\frac{\mathcal{P}^Q_{jmn}}{\omega_j^2})^2 + W'_3(\mathcal{V}^Q_{jmn})^2]\rangle \\
& \quad + \sum_{j=1}^{n_c} 8[z'_{jm}z'_{jn}(\frac{\mathcal{P}^C_{jmn}}{\omega_j^2})^2 + a'_{jm}a'_{jn}(\mathcal{V}^C_{jmn})^2 \\
& \quad + (a'_{jn}z'_{jm} - a'_{jm}z'_{jn})(\frac{\mathcal{P}^Q_{jmn}}{\omega_j^2})^2] \\
& \quad + \sum_{j=1}^{n_c-1}\sum_{k=j+1}^{n_c}\langle 8[X'_{j2}(\frac{\mathcal{P}^C_{jmn}}{\omega_j^2})^2 + Y'_{j2}(\mathcal{V}^C_{jmn})^2 + X'_{k2}(\frac{\mathcal{P}^C_{kmn}}{\omega_k^2})^2 \\
& \quad + Y'_{k2}(\mathcal{V}^C_{kmn})^2] + 8[X'_{j3}(\frac{\mathcal{P}^Q_{jmn}}{\omega_j^2})^2 + Y'_{j3}(\mathcal{V}^Q_{jmn})^2 \\
& \quad + X'_{k3}(\frac{\mathcal{P}^Q_{kmn}}{\omega_k^2})^2 + Y'_{k3}(\mathcal{V}^Q_{kmn})^2]\rangle\} \qquad (3.84)
\end{aligned}
$$

In this expression, $\mathcal{P}^A_{jm}$ and $\mathcal{V}^A_{jm}$ are the mth auto floor spectra for the pseudo acceleration and relative velocity response, respectively, of a second order oscillator; $\mathcal{P}^C_{jmn}$, $\mathcal{V}^C_{jmn}$, and $\mathcal{P}^Q_{jmn}$, $\mathcal{V}^Q_{jmn}$ represent the associated cross floor response spectra between the mth and nth inputs corresponding to the coincident and quadrature

components,and $\mathcal{Z}^{A}_{jm}$, $\mathcal{Z}^{C}_{jmn}$, $\mathcal{Z}^{Q}_{jmn}$ denote the auto and cross floor spectra for the relative velocity response of a first order massless system. Using equation (3.84) we can calculate the design response of a rotating machine sitting on the floor of a building which is subjected to seismic base motions.

3.5 Summary

Equations (3.59) and (3.77) provide the expressions for calculating the mean square response by the stochastic analysis for seismic inputs defined in terms of spectral density functions. In equation (3.59) the spectral density functions are for the principal excitation components, whereas in equation (3.77) the spectral density functions are for the floor motions. To obtain these floor spectral density functions, one must analyze the primary structure for seismic excitations applied at its base. These equations will be used in the following chapter to obtain numerical results for the mean square response of a rotor system in a parametric study.

Equations (3.83) and (3.84), on the other hand, provide the expressions for calculating the design response by the response spectrum approach. In equation (3.83) the input spectra of the base excitations are for the principal components, whereas in equation (3.84) the input spectra are for the floor motions. These latter spectra are defined in terms of the auto and cross response spectra of various components of the motions of a floor on which the rotating machine is placed. These spectra are obtained from the analysis of the supporting structure, as described by Singh and Burdisso (1987). These response spectrum expressions have also been used in the following chapter to compute the design rotor response.

Chapter 4

Numerical Results

4.1 Introduction

In this chapter, we present some numerical results for an example problem of a shaft-disk-bearing system using the equations developed in the previous chapter. The expressions for calculating rotor responses given in Chapter 3 are quite general. These expressions include both the real and complex eigenproperties of the system and individually identify their contributions to a response quantity. Also the effects of the rotational acceleration and rotational velocity inputs on the total response have been separated out from those of the translatonal components. Here we will use these expressions to numerically evaluate the contributions of these different terms to a response quantity to examine if any terms can be deleted to simplify the analysis. In particular, we will evaluate how important the terms associated with the real eigenproperties are. We will also investigate under what situations the contribution of the rotational components is significant. In the development of the response spectrum approach in the preceding chapter, simplifying assumptions such as stationarity of the earthquake input and system response and equality of the peak factors were made.

In this chapter we will also verify the applicability of the proposed response spectrum method developed with such assumptions by a numerical simulation study.

4.2 Example Rotor-Bearing System

To obtain the numerical results, the rotor-bearing system shown in Figure 4.1 has been considered. This rotor system was also used by Earles et al. (1987) and Suarez et al. (1992) in their numerical example. The physical and mechanical properties of this system are given in Table 4.1. The rotor operates at a spinning speed of 880 rpm which is well below the instability speed of 2295 rpm. To analyze this system, the shaft was discretized into 14 finite elements. The displacement field over each element was defined by the cubic beam interpolation functions. The total number of degrees of freedom of this example problem is 60.

This rotating system was analyzed to obtain its eigenvalues and left and right eigenvectors. A first few frequencies and damping ratios of the system are shown in Table 4.2. These eigenproperties were used in the calculation of numerical results. The response values have been obtained for the two displacements D_x and D_y of the disk and for two force components F_x and F_y at one of the two bearings in the horizontal and vertical directions.

4.3 Seismic Inputs

Stochastic Inputs

The stochastic models for the principal components of the ground motion were defined by the three-term Kanai-Tajimi spectral density functions of the following form:

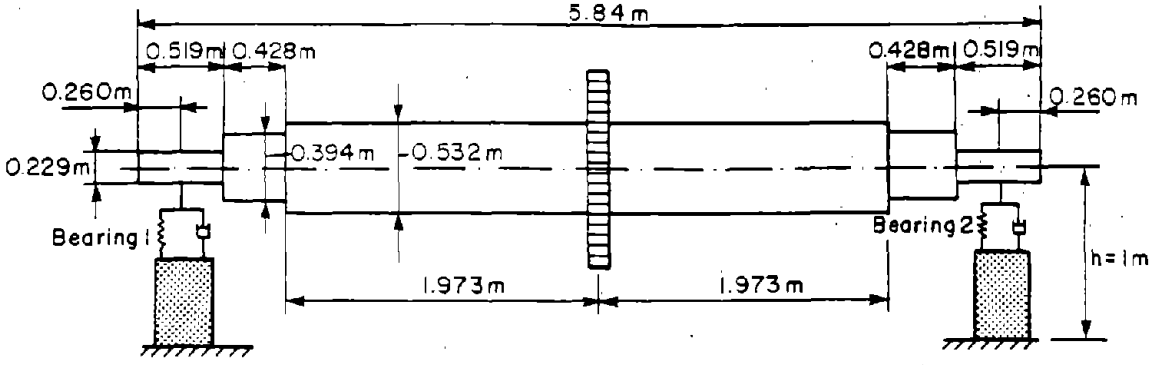

Figure 4.1: Configuration of the rotor system considered for study

Table 4.1: Physical and mechanical properties of the rotor

Disk mass, m_d	=	5670 kg
Transverse moment of inertia, I_x	=	3550 kg·m^2
Polar moment of inertia, I_p	=	7100 kg·m^2
Mass density of shaft, ρ	=	7806 kg/m^2
Modulus of elasticity, E	=	2.078×10^{11} N/m^2
Poisson's ratio, ν	=	0.3
Revolutions per minute, N	=	880 rpm
Viscosity, μ	=	0.14839 N·s/m^2
Diameter of journal, D	=	0.229 m
Length of journal, L	=	0.229 m
Clearance, C	=	3.8×10^{-4} m
Weight of bearing, W	=	67120 N
Bearing stiffness coefficients at opearating speed 880 rpm in N/m		
$K_{xx} = 0.18305 \times 10^9, K_{xy} = 0.37487 \times 10^9$		
$K_{yx} = -0.72481 \times 10^9, K_{yy} = 0.10977 \times 10^{10}$		
Bearing damping coefficients at opearating speed 880 rpm in N·s/m		
$C_{xx} = 0.54139 \times 10^7, C_{xy} = 0.17090 \times 10^7$		
$C_{yx} = C_{xy}, C_{yy} = 0.21294 \times 10^8$		

Table 4.2: Frequencies and damping rations for the first 10 modes of the example rotor system

Mode no.	Frequency (cps)	Damping ratio (%)
1	10.3965	71.46
2	10.7882	69.12
3	23.3762	9.53
4	24.0083	1.98
5	79.8363	2.87
6	97.1774	3.01
7	210.9122	0.97
8	211.0740	4.00
9	220.1107	1.75
10	229.5606	1.58

$$\hat{\Phi}_l(\omega) = \sum_{i=1}^{3} s_{il} \frac{\omega_{il}^4 + 4\beta_{il}^2\omega_{il}^2\omega^2}{\left(\omega_{il}^2 - \omega^2\right)^2 + 4\beta_{il}^2\omega_{il}^2\omega^2} \qquad -\omega_c \leq \omega \leq \omega_c \quad l = 1,2,3 \qquad (4.1)$$

where s_{il}, ω_{il}, and β_{il} are the ground parameters for the translational acceleration component in the lth principal direction and ω_c is the cutoff frequency. These parameters are given in Table 4.3. This spectral density function, which represents a broadband seismic input, has also been used in several earlier studies. The first and third principal directions are assumed to have the same spectral density function parameters, and the characteristics of the second component are assumed to be different. In particular, the root mean square value of the excitation along the second direction is 2/3 of the other two components. With these parameter values, the maximum ground acceleration level is about $0.2g$ for the first and third components, and for the second principal excitation it is $0.134g$, which is 2/3 the magnitude in the other two directions. Equation (4.1) was directly used to obtain the frequency integrals in the stochastic analysis to calculate the rotor response.

Time History Inputs

For verification of the response spectrum approach developed in this work, an ensemble of time histories have been used in the simulation study. These ground motion time histories were generated for the stochastic input motion defined by equation (4.1). To generate the acceleration time histories the following superposition of harmonic waves with random phase, as proposed by Rice (1954) and Shinozuka (1987), has been used here:

$$\ddot{X}_l(t) = \sum_{m=1}^{N_f} \sqrt{4\hat{\Phi}_l(\omega_m)\Delta\omega}\cos(\omega_m t + \phi_{ml}) \qquad (4.2)$$

where $\ddot{X}_l(t)$ is the acceleration of the lth component; ϕ_{ml} is the random phase angle; $\Delta\omega$ is the frequency increment and N_f is the number of harmonics which the cutoff frequency range is divided into. Since the three principal excitations are uncorrelated,

Table 4.3: Parameters of the spectral density function for three principal components

lth excitation	i	s_{il} ($m^2 \cdot s/rad \times 10^{-3}$)	ω_{il} (rad/s)	β_{il}
1	1	1.908	13.500	0.3925
	2	0.630	23.500	0.3600
	3	0.477	39.000	0.3350
2	1	0.848	16.875	0.3925
	2	0.280	29.375	0.3600
	3	0.212	48.750	0.3350
3	1	1.908	13.500	0.3925
	2	0.630	23.500	0.3600
	3	0.477	39.000	0.3350

$\omega_c = 30$ cps

here, three different sets of independent random phase numbers, which are uniformly distributed in the range of $(0, 2\pi)$, generated by the computer along with the parameter $N_f = 600$ were used to create the acceleration time histories corresponding to the given spectral density functions. The ground motion produced according to equations (4.1) and (4.2) was then modulated by a deterministic envelope to simulate the build-up, strong motion, and decay stages usually observed in earthquake records. In this study, an ensemble of 50 sets of accelerograms with duration lasting 24 seconds were synthetically constructed. Each set consisted of two equal intensity components and one lower intensity component. Figure 4.2 shows a typical sample group of translational acceleration records of the three principal components. For the generated time histories, a 2-seconds parabolic build-up phase, a strong motion phase of 10 seconds with amplification factor equal to one, and an exponentially attenuated decay phase of 12 seconds have been used to define the envelope function.

Response Spectra Inputs

The synthesized time histories were used to define the pseudo acceleration and relative velocity ground response spectra for the principal components of excitation. A step-by-step recursive algorithm developed by Nigam and Jennings (1969) was employed to process the time histories. The design spectra were defined as the mean and mean-plus-one-standard-deviation spectra of the time history ensemble. Figures 4.3 and 4.4 show the mean pseudo acceleration and relative velocity response spectra of the first and third principal components. These mean spectra for the second principal component are shown in Figures 4.5 and 4.6. They are plotted for oscillator periods from 0.01 to 50 seconds with damping ratios of 0.005, 0.01, 0.02, 0.03, 0.04, 0.05, 0.06, 0.08, 0.1, and 0.2. Figures 4.7 to 4.10 show the similar set of mean-plus-one-standard-deviation response spectra.

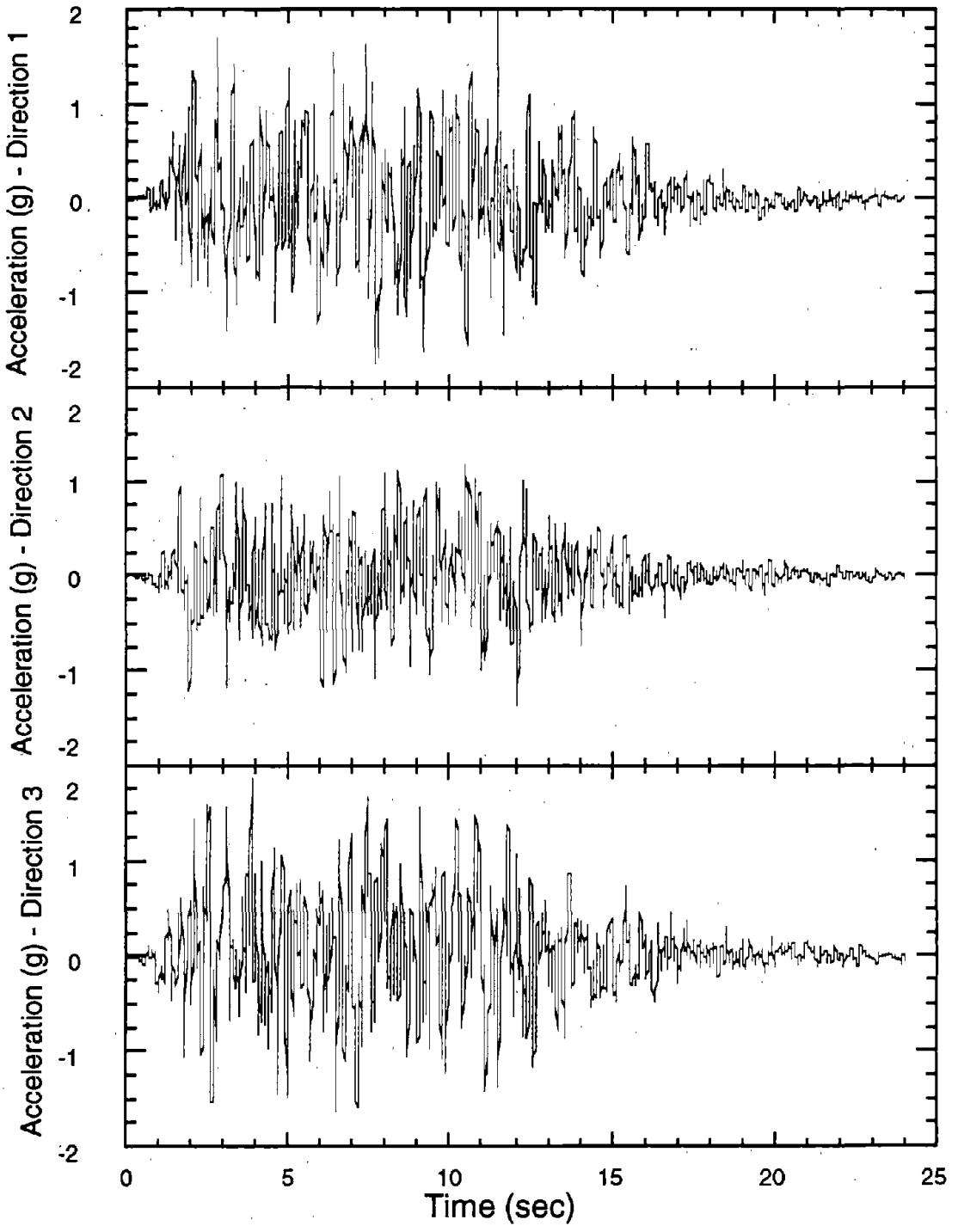

Figure 4.2: A sample group of generated acceleration time histories along three principal directions

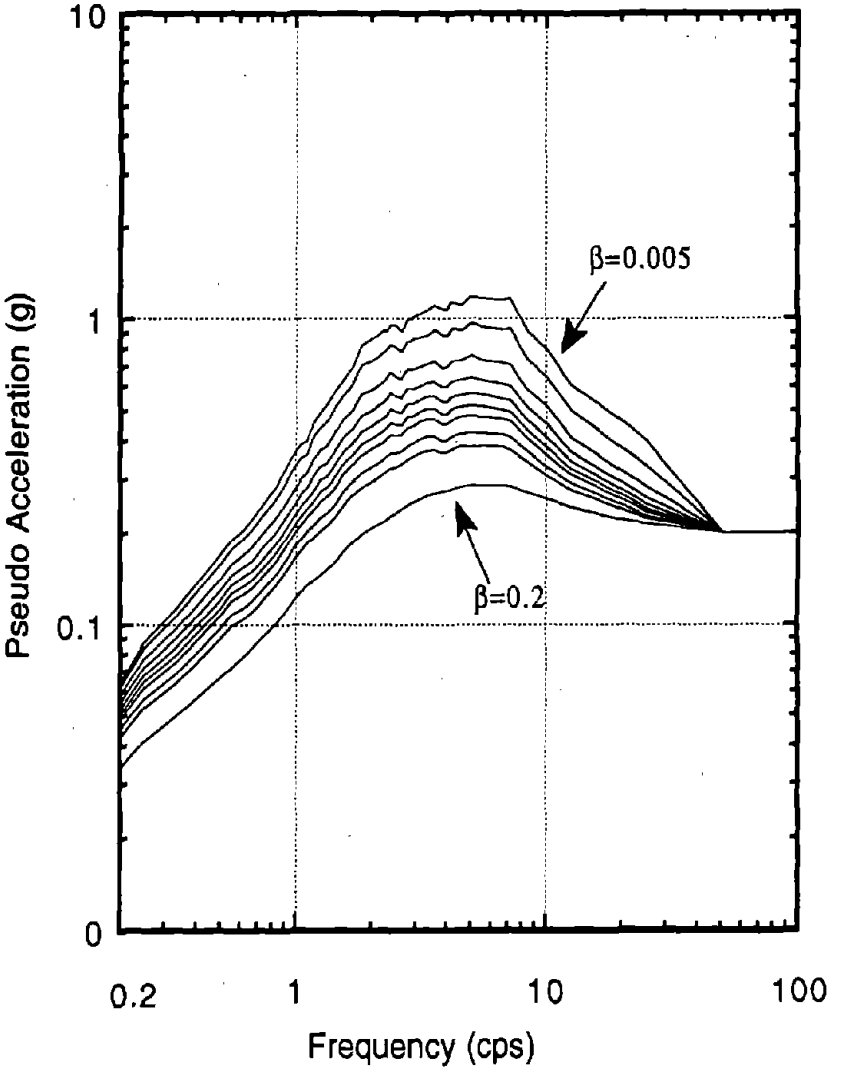

Figure 4.3: Mean pseudo acceleration response spectra of the major principal excitation component for the ensemble of ground motions considered in the study.

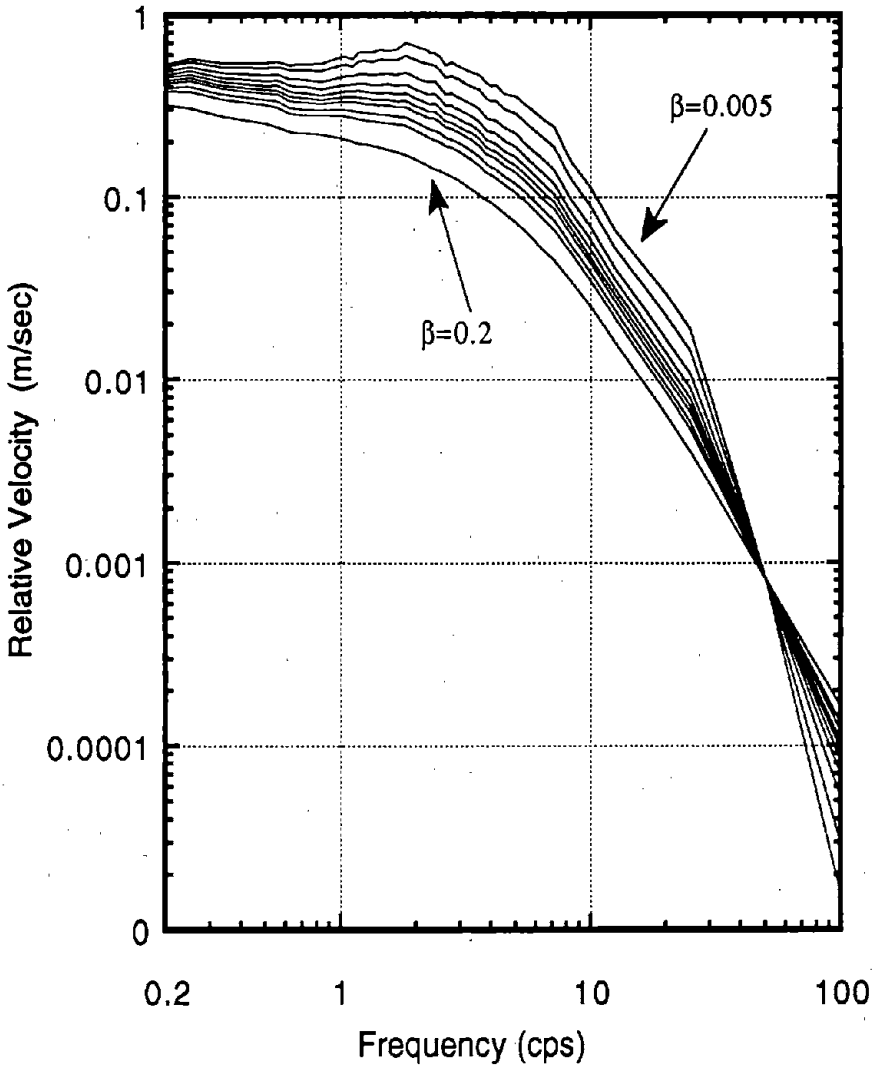

Figure 4.4: Mean relative velocity response spectra of the major principal excitation component for the ensemble of grounf motions considered in the study.

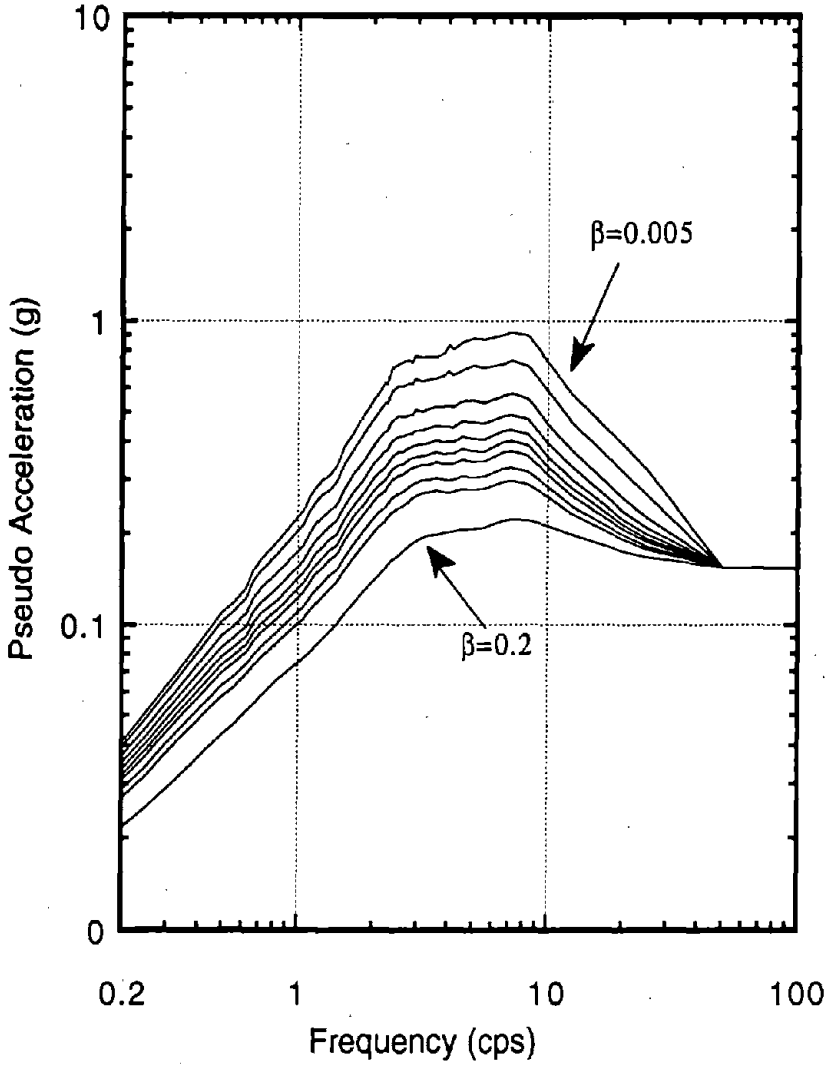

Figure 4.5: Mean pseudo acceleration response spectra of the minor principal excitation component for the ensemble of ground motions considered in the study.

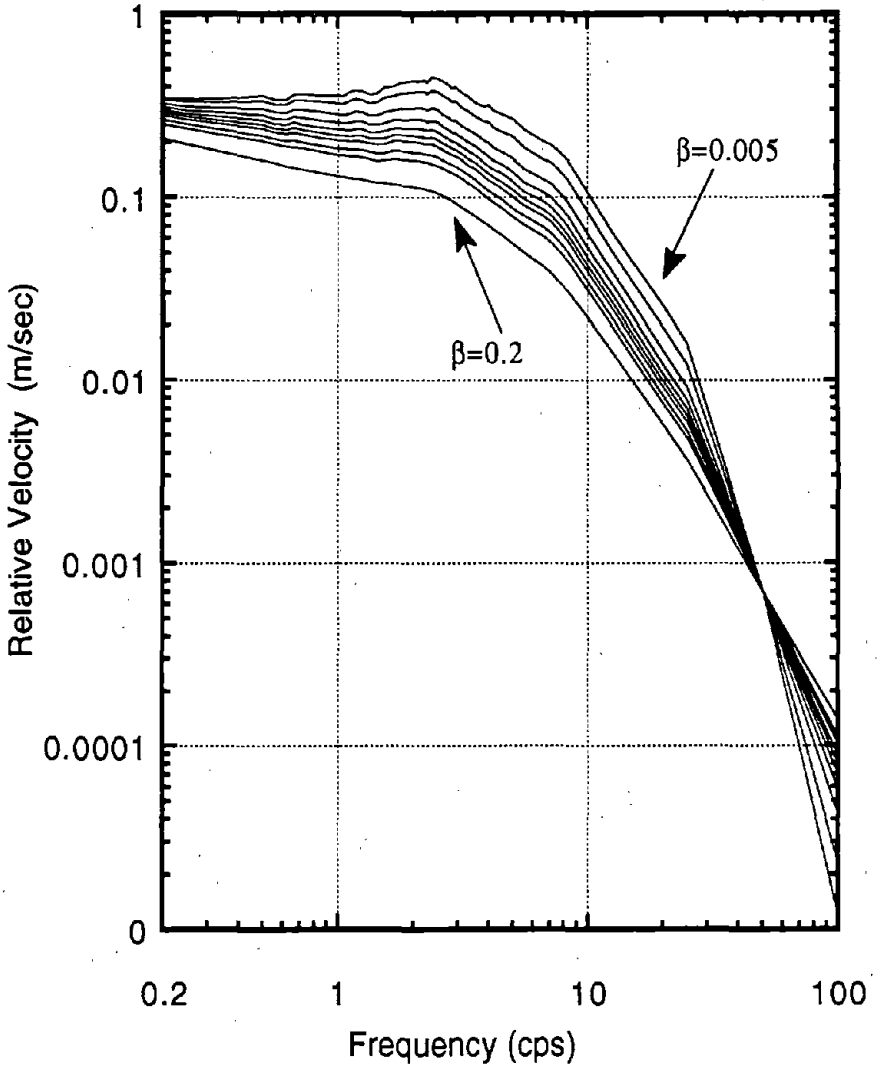

Figure 4.6: Mean relative velocity response spectra of the minor principal excitation component for the ensemble of ground motions considered in the study.

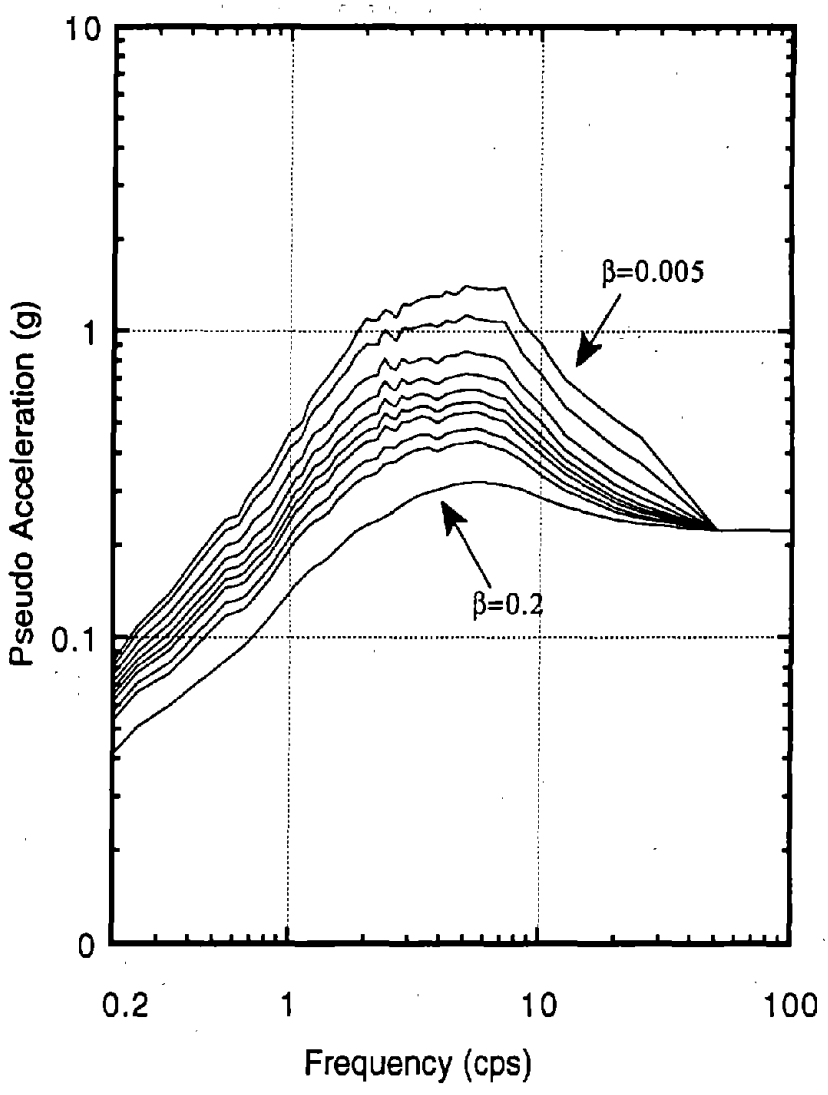

Figure 4.7: Mean-plus-one-standard-deviation pseudo acceleration spectra of the major principal excitation component for the ensemble of ground motions.

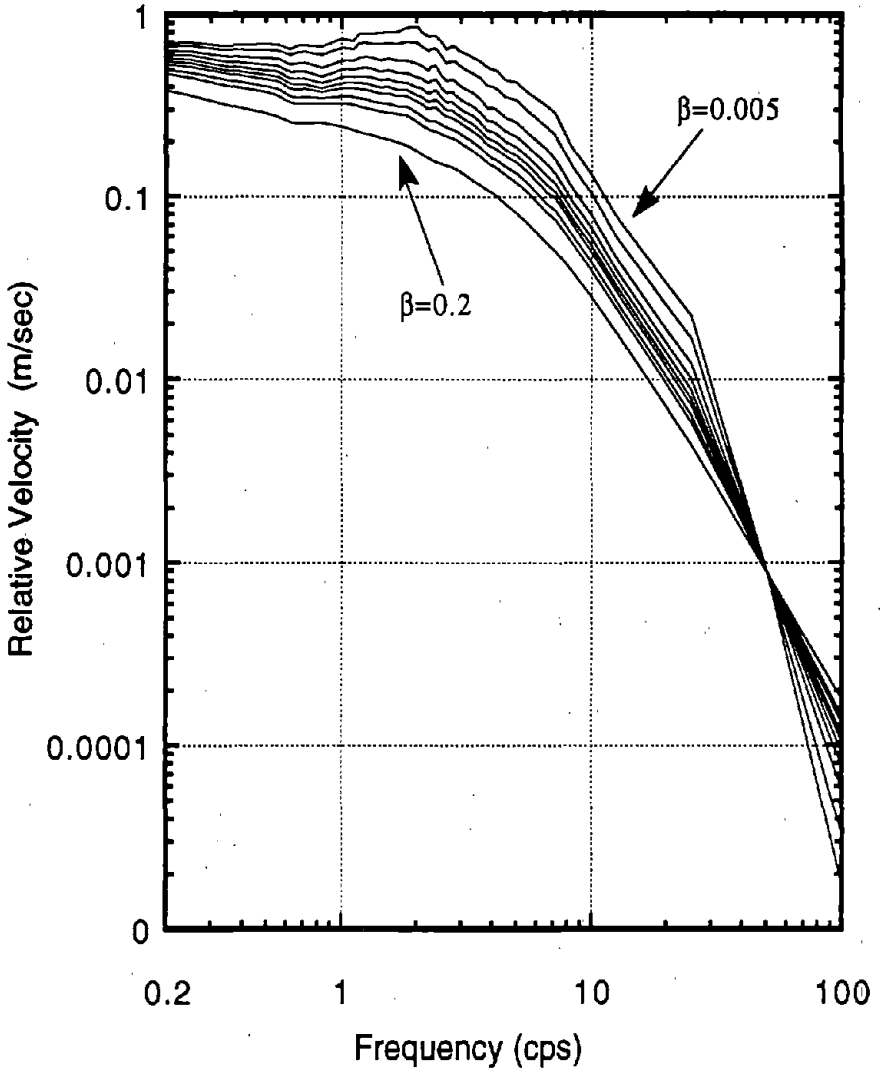

Figure 4.8: Mean-plus-one-standard-deviation relative velocity spectra of the major principal excitation component for the ensemble of ground motions.

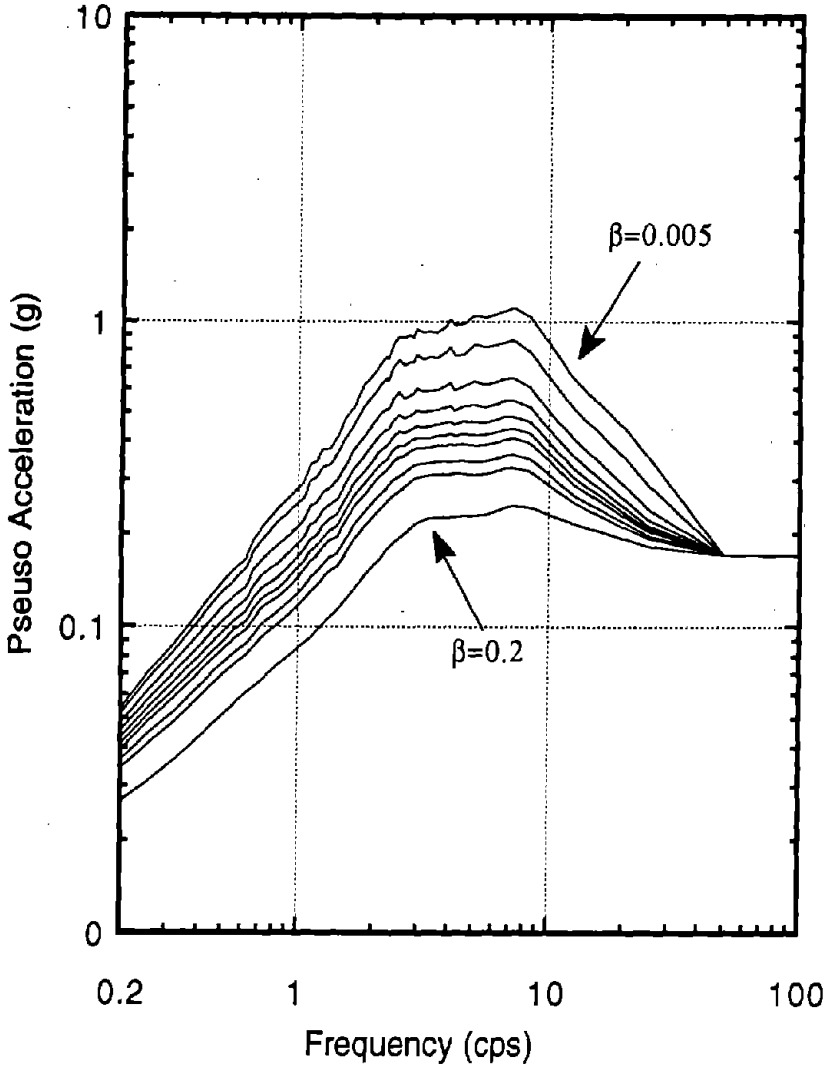

Figure 4.9: Mean-plus-one-standard-deviation pseudo acceleration spectra of the minor principal excitation component for the ensemble of ground motions.

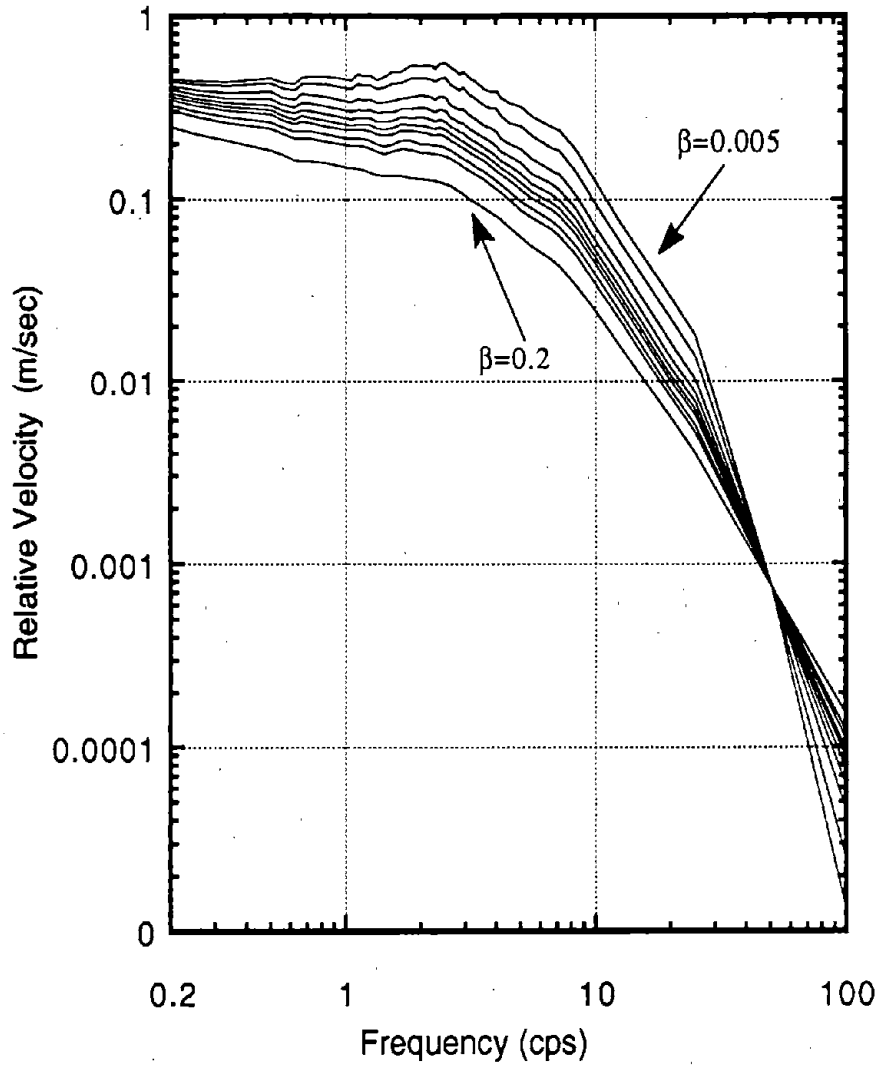

Figure 4.10: Mean-plus-one-standard-deviation relative velocity spectra of the minor principal excitation component for the ensemble of ground motions.

In the response spectrum analysis with the travelling seismic wave model, these ground response spectra were used to define the base inputs. The details of the verification of the proposed spectrum approach are provided later in Section 4.5. To study the influence of the rotational base inputs of a rotor sitting on a building floor, these ground response spectra were applied at the base of the building as the seismic inputs to obtain the the correlated floor response spectra. These calculated floor response spectra were then used as the base inputs to the rotor system to calculate its design response. This analysis is covered in Section 4.6.

4.4 Contribution of Real Eigenproperties

A rotor-bearing system will usually have some real eigenvalues. For the example rotor studied here, which is supported on fluid film bearings, there were exactly four real eigenproperties. They exist due to the highly damped characteristics of the journal-bearing system. It was obsereved from the modal analysis results that the frequencies corresponding to these real eigenvalues were very high. They can be considered to represent overdamped or critically damped modes. Since for earthquake type ground motions, the integral (J_{0l_j}) decreases very fast with inceasing frequency (α_j), it was suspected that the contribution of the terms associated with the real modes to a response quantity was not going to be significant.

Because the formulation developed in the previous chapter separated the effect of the real eigenproperties from that of the complex eigenproperties, it was quite simple to ascertain their contribution by including or neglecting the terms associated with these modes in the response calculation. In Table 4.4, we show the root mean square response values obtained for the stochastic inputs without rotational

components. These response results were calculated with and without the real eigenproperty associated terms. It is observed that the effect on the total response of the real eigenproperties is, indeed, small as the difference in the results is less than 1.5%. Similar results were also observed when the rotational input components were included. In further analysis, therefore, the contribution of the terms associated with real eigenvalues is ignored; only the terms associated with the complex modes have been used to calculate the rotor responses.

4.5 Verification of Response Spectrum approach

To verify the applicability of the response spectrum approach proposed in this work, here a numerical simulation study is conducted. In this study, the response values obtained from the time history analyses used as the benchmark are compared with the response values obtained by the response spectrum method. We consider the case in which the rotational inputs are absent.

In the response spectrum approach, the design response values are obtained by utilizing equations (3.80) and (3.83) for the input response spectra defined in Section 4.3. To obtain the mean values of the design response, the mean spectra shown in Figures 4.3, 4.4, 4.5 and 4.6 were used as the base inputs. Likewise, to calculate the mean-plus-one-standard-deviation values of the design response, the response spectra shown in Figures 4.7, 4.8, 4.9 and 4.10 were utilized as the base excitations. The worst-case design response values were obtained when the principal excitations were applied along the rotor axes. In particular, the second principal component was oriented in the axial direction of the rotor (z axis), while the other two components were applied, interchangeably, along the transverse axes. In the time history analysis also,

Table 4.4: Rotor responses including and excluding real modes by stochastic analysis

Response	With real modes	Without real modes	Diff. (%)
D_x (mm)	0.0454	0.0454	0.0
D_y (mm)	0.0468	0.0468	0.0
F_x (kN)	4.9515	4.8850	-1.3
F_y (kN)	6.1222	6.0755	-0.8

the response values were calculated for each set of accelerograms applied along these same directions to ensure that the seismic inputs in both approaches are consistently applied.

To obtain the response in the time history approach, the generalized modal superposition method was used. The uncoupled modal equations (3.7) were solved by a step-by-step recursive procedure. For discretized base motion inputs $E_i(t)$ which is assumed to be linear between consecutive time steps t_{k-1} and t_k, the solution of the principal coordinate q_j can be expressed as follows:

$$q_j(t_k) = e^{\lambda_j \Delta t}[q_j(t_{k-1}) + \frac{Q_{1j}}{\lambda_j^2}] - \frac{Q_{2j}}{\lambda_j^2} \tag{4.3}$$

where

$$\begin{aligned} Q_{1j} &= \sum_{i=1}^{n_e} \{\psi_L\}_j^T \{r\}_i (h_i + \lambda_j h_{oi}) \\ Q_{2j} &= \sum_{i=1}^{n_e} \{\psi_L\}_j^T \{r\}_i [h_i + \lambda_j (h_{oi} + h_i \Delta t)] \\ h_{oi} &= E_i(t_{k-1}) \\ h_i &= \frac{1}{\Delta t}[E_i(t_k) - E_i(t_{k-1})] \end{aligned}$$

in which Δt is the time step and other quantities have been defined in chapter 3. Here the forcing components E_1, E_2, and E_3 are the base inputs along the directions of rotor axes x, y, and z, which, as mentioned earlier, correspond to the first (or the third), the third (or the first), and the second principal excitation components. In terms of the time history of the principal coordinates defined above, a response quantity at time t_k can be obtained from equation (3.10) as:

$$S(t_k) = \sum_{j=1}^{2n_t} \{T\}^T \{\psi_R\}_j q_j(t_k) \tag{4.4}$$

Using equation (4.4), the time histories of the response quantities of interest were obtained for the 50 sets of generated accelerograms. Figure 4.11 shows the plot of a

sample response time history of the disk displacement obtained by this approach. For a response quantity, each of the time histories were scanned to obtain the maximum value. These maximum response values were then statistically processed to compute the ensemble mean and mean-plus-one-standard-deviation values of the maximum response. The mean and mean-plus-one-standard-deviation response values obtained for the time history ensemble are compared with the mean and mean-plus-one-standard-deviation response values obtained in the response spectrum approach.

These response values obtained by both the approaches are shown in Table 4.5. Considereing the response values by the time history analysis as the benchmark results, the percentage differences computed for all response quantities obtained by the spectrum approach are less than 6%. This variation is well within the range of the one-standard-deviation error bound. This excellent comparison of the results confirms the validity of the proposed response spectrum approach for calculating the design response of rotating machines, even though the approach is based on the assumptions of the stationarity of the input and response and the equality of peak factors, as discussed in Chapter 3.

4.6 Effect of Rotational Inputs

Even though it is a common practice to neglect the rotational components of the inputs in seismic response analysis of structures, there are some situations in which rotating machines may be exposed to rotational base motions. It is, thus, of interest to evaluate the relative importance of the rotational input terms in the forcing function on the rotor response. Since the effects from different input components were separated in the response expressions developed in the previous chapter, it is quite

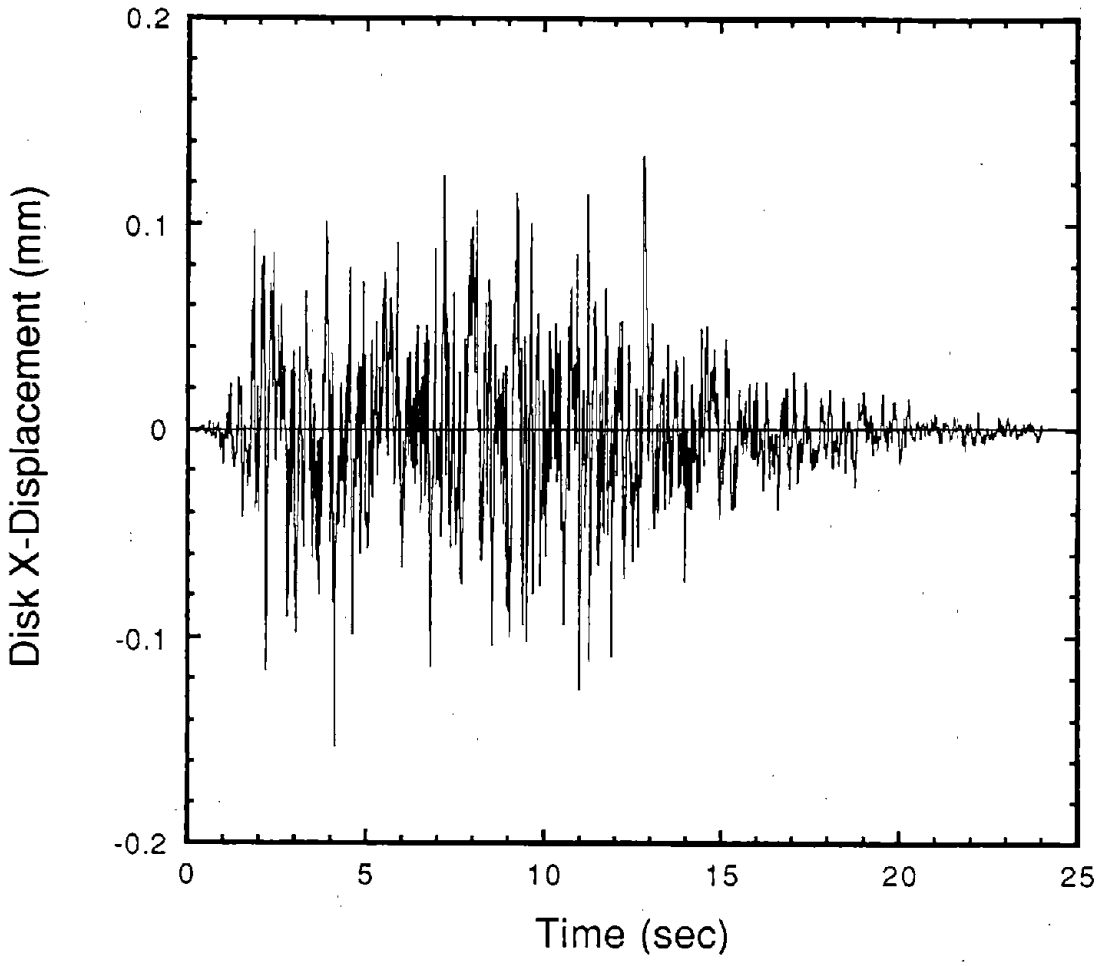

Figure 4.11: Response time history of the disk displacement of the rotor in the x direction by the modal time history analysis

Table 4.5: Comparison of the maximum rotor responses obtained by the spectrum and time history analyses for the mean and mean-plus-one-standard-deviation responses

Mean Response

Response	Spectrum result	Time history result	C.O.V.	Difff. (%)
D_x (mm)	0.1425	0.1430	0.0681	-0.35
D_y (mm)	0.1491	0.1440	0.1074	3.54
F_x (kN)	15.235	15.646	0.0709	-2.63
F_y (kN)	19.343	18.940	0.1004	2.13

Mean-plus-one-standard-deviation Response

Response	Spectrum result	Time history result	Diff. (%)
D_x (mm)	0.1512	0.1527	-0.98
D_y (mm)	0.1685	0.1595	5.64
F_x (kN)	16.125	16.755	-3.76
F_y (kN)	21.855	20.841	4.86

simple to evaluate the relative contribution of the rotational input components. In this section we will examine this for both types of input models—the seismic wave and cross correlation matrix models.

4.6.1 Seismic Wave Model

In this model, we will evaluate the contribution of the rotational components of increasing intensity level to the rotor response. In the seismic wave model, the intensity of the rotational input can be easily changed by varying the apparent wave velocity, c. As the wave velocity appears in the denominator of equation (3.19), the lower the wave velocity, the higher the magnitude of the rotational components. Here five values of the wave velocity ranging from 10 m/sec to 800 m/sec were arbitrarily selected. The rotational components corresponding to the wave velocity of 10 m/sec are very strong. However, it is mentioned that such low wave velocities are not expected in any engineering foundation of structures. Since it is expected that a higher pedestal will amplify the rotational effect felt by the machine, the rotor pedestal height has also been changed to study the effect of the base rotation on the response bahavior.

Effect of rotational acceleration terms

The root mean square values of the rotor response calculated with and without the rotational accelerations (but no rotational velocities) inputs included in the analysis are given in Table 4.6. These results were obtained for a rotor at different heights subjected to the seismic wave excitations with different wave velocities. The contribution of the rotational acceleration terms can be evaluated by comparing these response values with the results calculated without any rotational inputs, which correspond to $c = \infty$. For h =0 m, the displacements of the disk remained the same

Table 4.6: Rotor responses by stochastic analysis using the seismic wave model for different wave velocities and rotor heights with rotational accelerations as rotational inputs

Response quantity	Rotor ht. h (m)	Results for wave velocity c (m/sec) c =10	c =30	c =100	c =300	c =800	$c = \infty$
D_x (mm)	0	0.0454	0.0454	0.0454	0.0454	0.0454	0.0454
	1	0.1974	0.0790	0.0497	0.0460	0.0455	0.0454
	3	0.5761	0.1974	0.0739	0.0497	0.0461	0.0454
D_y (mm)	0	0.0468	0.0468	0.0468	0.0468	0.0468	0.0468
	1	0.0737	0.0448	0.0447	0.0460	0.0464	0.0468
	3	0.2141	0.0737	0.0444	0.0447	0.0459	0.0468
F_x (kN)	0	6.8842	5.0107	4.8508	4.8677	4.8779	4.8850
	1	22.523	8.7371	5.3122	4.9225	4.8861	4.8850
	3	67.323	22.889	8.2824	5.3618	4.9518	4.8850
F_y (kN)	0	7.8021	6.1709	6.0483	6.0616	6.0697	6.0755
	1	9.9473	5.6545	5.7244	5.9395	6.0224	6.0755
	3	26.531	8.8507	5.5116	5.7383	5.9335	6.0755

regardless of the wave velocity, whereas the forces at the bearings were observed to increase about 40% in the x direction and 28% in the y direction for very strong rotational inputs. In the cases where the rotor base was elevated, the responses in the horizontal direction grew steadily with the rotational intensity. At the highest intensity of the rotational input, both the displacement and bearing force values increased about 3.5 times for h =1 m and almost 12 times for rotor height of 3 m. The responses along the vertical direction, however, are somewhat different. At first the response magnitudes are seen to decrease for the weaker intensities of rotational components, but then they increase continuously as the base rotations become stronger. Eventually both the disk displacement and bearing force grow to about 1.6 times for h =1 m and 4.5 times for h =3 m of the values obtained without base rotations.

To better illustrate how the rotor response varies with parameters c and h, these results are also plotted in Figure 4.12 and 4.13. It is obvious from these figures that, in general, the response of a rotor increases with the intensity of the base rotation. It is also noted that the response curves of h =3 m rise much faster than the curves for the other two smaller rotor heights. This implies that increasing the height of the rotor base enhances the effect of the rotational inputs, especially at high rotational intensities. These results indicate that the contributions of the input rotational components to the response can be high if the rotational excitations are strong and the rotor is placed on a raised pedestal. However, for the apparent wave velocities of 300 m/sec to 800 m/sec, which are more likely to be encountered in normal soil stratum for supporting engineering structures, the relative effect of the rotational components is seen to be rather insignificant. Thus for rotors directly placed on a firm foundation, the contribution of the rotational components can be conveniently neglected without affecting the accuracy of the calculated response.

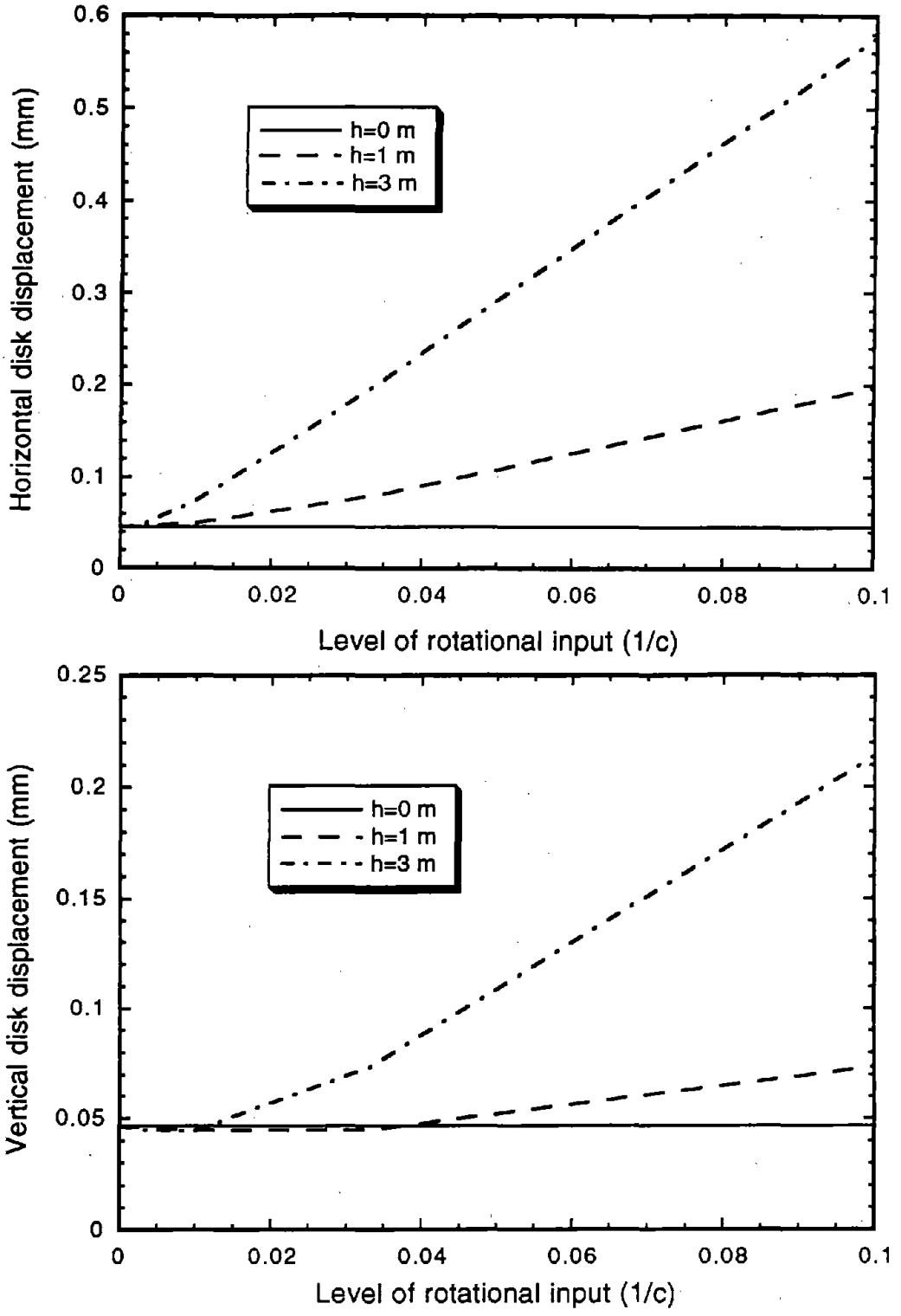

Figure 4.12: Response of the disk displacements for various seismic wave velocities and rotor heights

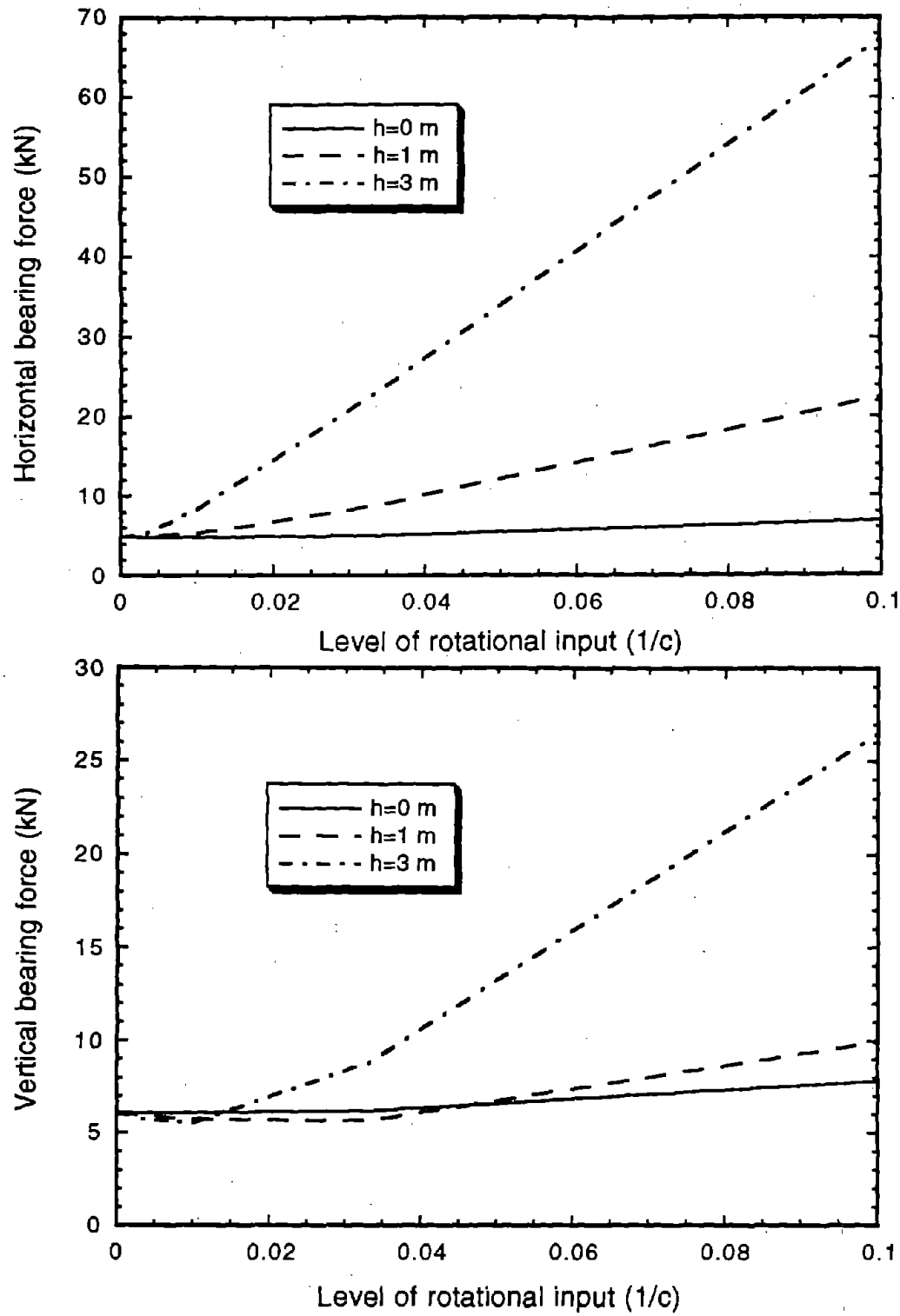

Figure 4.13: Response of the bearing forces for various seismic wave velocities and rotor heights

Effect of rotational velocity terms

As some of the forcing function terms also depend upon the rotational base velocities, and since they complicate the seismic input description in the calculation of response by the response spectrum approach, it is also of interest to examine the relative contribution of these terms to see if they can be neglected to simplify the analysis. To study this, the mean square response expression which included all parts of the forcing function—translational accelerations, rotational accelerations and rotational velocities—was utilized. Here again, since in the final expression the effect of the velocity dependent terms was separated, it was quite simple to delete these terms to evaluate their importance. The results obtained with and without these velocity terms are shown in Table 4.7. The percentage difference shown in the table for various wave velocities and rotor heights was calculated using the response value obtained without the rotational velocity inputs as the benchmark. The response results of the disk displacements for these two sets of seismic inputs are virtually identical. The bearing force response values show only slight disparity, about 5% at most among all the cases. Thus it is apparent that the contribution of the rotational velocity terms to the total response of a rotating machine is not significant. To simplify the analysis, therefore, these rotational velocity components can also be compleltely ignored without affecting the accuracy of the calculated response.

4.6.2 Correlation Matrix Model

Another situation in which a rotating machine can experience rotational excitations at its base is through its supporting structure, even though there may not be any significant rotational components in the seismic motion which excites the supporting structure. To examine what effect such rotational excitations coming from

Table 4.7: Rotor responses by stochastic analysis including the rotational velocity as well as acceleration terms as base rotational inputs

Response quantity		$h = 1$ m c =10	c =100	c =300	$h = 3$ m c =10	c =100	c =300
D_x (mm)	result	0.1974	0.0496	0.0460	0.5761	0.0739	0.0496
	diff. (%)	0.0	0.0	0.0	0.0	0.0	0.0
D_y (mm)	result	0.0737	0.0447	0.0460	0.2141	0.0444	0.0447
	diff. (%)	0.0	0.0	0.0	0.0	0.0	0.0
F_x (kN)	result	23.495	5.3511	4.9269	67.814	8.3203	5.3681
	diff. (%)	4.3	0.7	0.1	0.7	0.5	0.1
F_y (kN)	result	10.475	5.7515	5.9422	27.165	5.5409	5.7412
	diff. (%)	5.3	0.5	0.1	2.4	0.5	0.1

the response of a supporting structure will have on a rotating machine, here we considered an example of a rotor placed in a three degrees of freedom building which also responded in torsional mode. This one-floor structure consists of a rigid slab supported on columns and shear walls. The mass center of the slab is eccentrically placed with respect to the stiffness center of the system. Thus the floor has two orthogonal translational components in the horizontal plane and a rotational component about the vertical axis in its response. The magnitudes of the eccentricity along the two horizontal directions are 0.05 and 0.10 multiplied by the radius of gyration of the slab. The frequencies, damping ratios, participation factors and mode shapes of this structure are given in Table 4.8.

The response of this supporting structure was obtained for the ground response spectra generated in Section 4.3. The mean spectra were used as the seismic inputs at the base of the building. The two horizontal excitations have equal intensities of maximum aceeleration $0.2g$, while the input in the vertical direction is 2/3 as strong as the horizontal components with maximum acceleration value of $0.134g$. As commonly assumed in the regular seismic analysis, the input components for the supporting structure were all translational and uncorrelated. The floor spectra were calculated through the dynamic analysis of the primary structure using the approach presented by Singh and Burdisso (1987). The motion of the slab has four components, two translations in the horizontal plane and a rotation in the vertical direction correlated with each other, along with the vertical translation which, assumed to reach the floor unfiltered, is the same as the ground vertical input and is uncorrelated with the other three components. These floor spectra, which comprise of the auto, coincident and quadrature spectra were then applied to the rotor as the base inputs.

Table 4.8: Dynamic properties of the supporting structure in which the rotor is placed

Mode no.	Freq. (rad/s)	Damping ratio	Participation factor x	y	θ_z	Mode shape ($\times 10^{-5}$) x	y	θ_z
1	8.7531	0.05	44.48	-26.11	0.0	8.555	-5.021	69.160
2	15.696	0.05	-3.38	-720.6	0.0	-0.65	-138.6	-2.495
3	20.031	0.05	719.7	-1.769	0.0	138.4	-0.340	-4.286

The maximum response of the machine was calculated for these input floor spectra by using equation (3.84). The rotor was oriented at different angles with respect to the axes of the slab. The height of the rotor base above the floor was set at 1 m. The results are shown in Figure 4.14 and 4.15. The design responses for both the displacements and bearing forces in the vertical direction display very little variation in the plots for different angles. The horizontal responses, however, have largest values when the rotor axis coincides with the structure axis with the lower eccentricity, and smallest values if the rotor axis is parallel to the structure axis with the higher eccentricity. It is also noted that the response values in the horizontal direction are always greater than those along the vertical direction, similar to what was observed in the wave model results. Analyses were also performed for excluding the rotational inputs. The response results from both cases are very close, with all differences being less than 1.2%. This shows that the contribution of the rotational inputs at the base is not significant. Since most buildings in practice are designed with as little rotational response as possible, the rotational excitation to a machine placed in such buildings is not likely to be any stronger than the rotational input considered in the above case. Thus, in such situations the contribution of the rotational base inputs is not expected to be very significant. These rotational excitation terms can, therefore, be ignored from any further design considerations. However, if it is desired the proposed response spectrum approach still permits us to include the rotational components in the seismic response analysis of rotating machines.

4.7 Summary

The response spectrum approach proposed in this work is verified by a simulation study. The mean and mean-plus-one-standard-deviation response values calculated

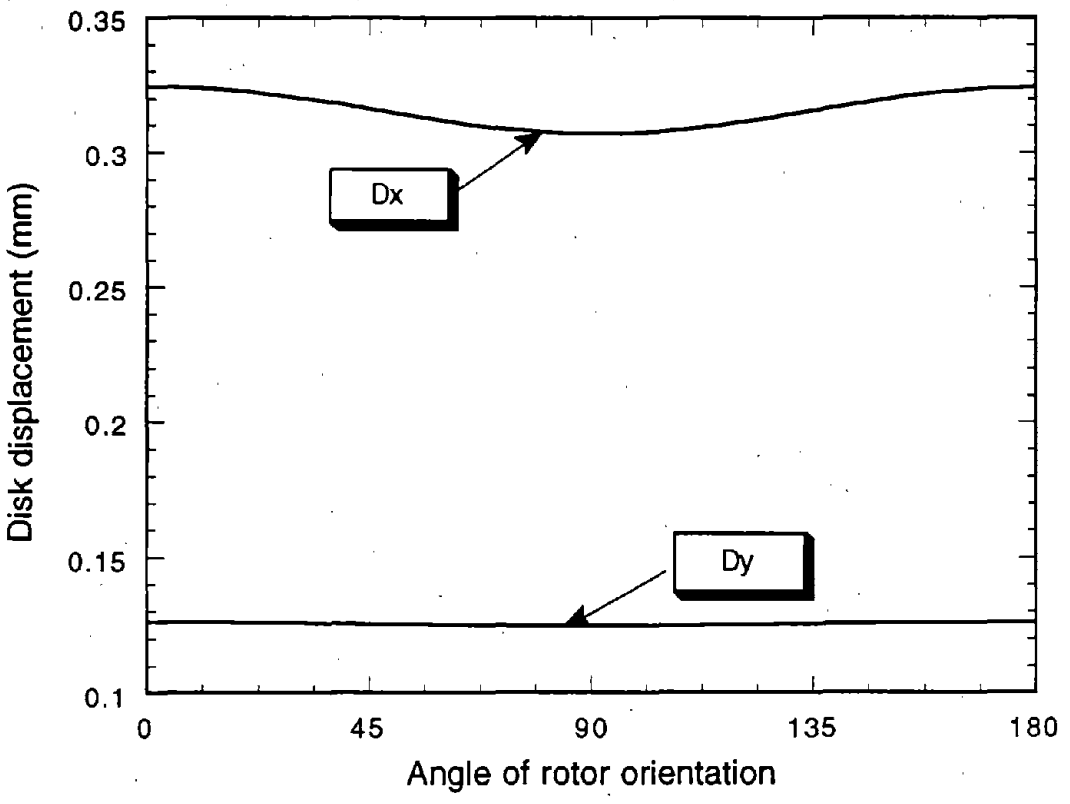

Figure 4.14: Response of the disk displacements using floor spectra as inputs in the correlation matrix model

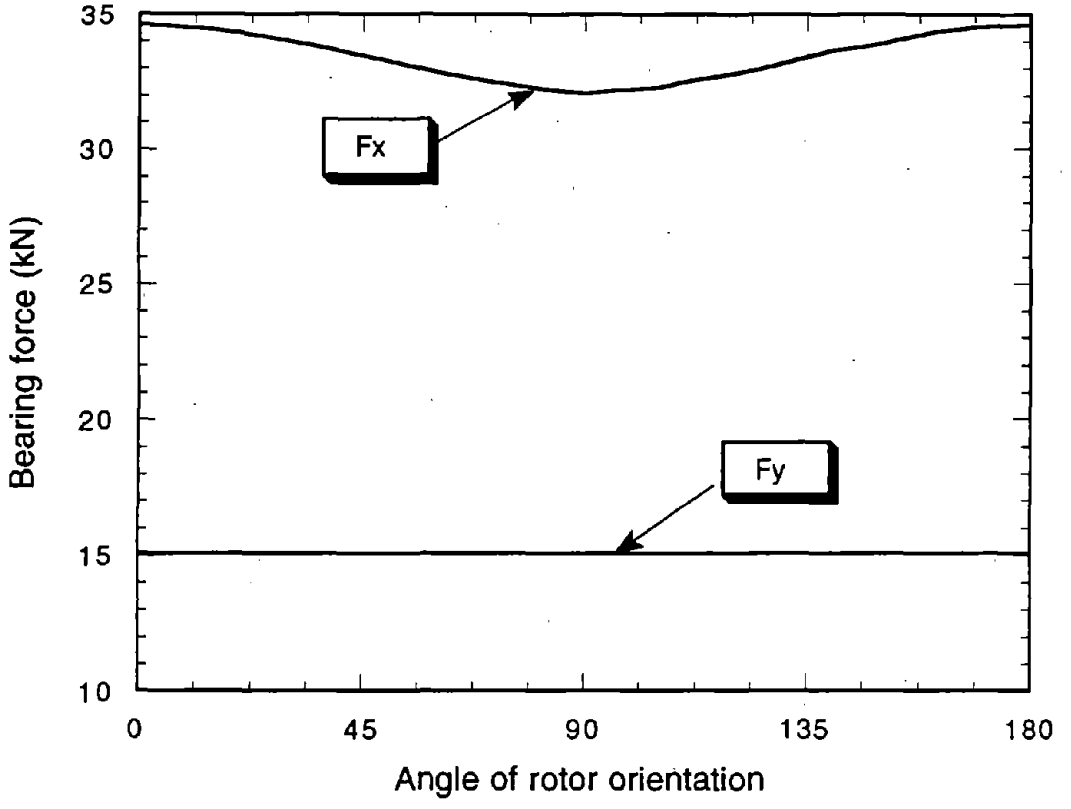

Figure 4.15: Response of the bearing forces using floor spectra as inputs in the correlation matrix model

by the response spectrum method are compared with the corresponding values calculated by the time history analysis for an ensemble of generated time histories. The difference in the two response values is well within the acceptable error range. This good comparison validates the reasonableness of the assumptions which were made regarding the peak factor equality and the stationarity of the input and response in the development of the spectrum approach.

The contribution of the real eigenproperties to the response of a rotating machine is also evaluated. The root mean square values of the response are obtained with and without the terms associated with the real modes. The comparison of the two response values calculated with and without real modes shows that the contribution of the terms associated with the real eigenproperties to the response is not significant. Thus, the terms associated with the real eigenproperties can be neglected in the analysis of a rotor-bearing system without affecting the accuracy of the calculated response.

The effect of the rotational base inputs on the rotor response is also examined in this chapter. The mean square response values are obtained for the travelling seismic wave model with rotational components of different intensity levels. Since the rotational effects may be amplified for a rotor placed high above its base, the rotor pedestals of different heights have also been considered. The effect of the rotational velocity components in the inputs is found to be unimportant. The rotational acceleration components of high intensities, on the other hand, can affect the response values noticeably, but such high intensity rotational excitations are rarely encountered in actual practice. The numerical results indicate that the rotational inputs to machines coming from the torsional response of the supporting structures are also not

expected to be strong enough to significantly affect a rotor response. Thus in practice the effect of the rotational base inputs can be ignored from any further consideration while calculating the response of a rotating machine. The proposed response spectrum approach, however, permits one to include the rotational components of the input as well if such components are considered to be strong.

Chapter 5

Closure

5.1 Concluding Remarks

Seismic response of rotating machines subjected to multi-component base excitations is studied. A rotating machine under earthquake loadings is a complex dynamic system to analyze. The equations of motion in their general form are difficult to solve. Fortunately, studies have indicated that, for seismic type of base motions, the problematic parametric terms in the system matrices and nonlinear forcing terms can be neglected. This enables one to develop an efficient response spectrum method for calculating the design response of rotating machines for seismic base inputs defined by input response spectra.

A formulation utilizing a generalized modal superposition approach with the random vibration analysis is presented to study the seismic response characteristics of rotating machines. The formulation is further extended to develop a response spectrum approach. The correlation between the excitation components are defined through two different models. In the first model, the correlation between the base excitation

components, including the rotational components, is expressed through the consideration of travelling wave effect. In the second model, the correlation is expressed through a correlation matrix. The expressions for both the travelling wave model and correlation matrix model are developed to calculate the response of rotating machines. In these expressions, the contribution of the real and complex real eigenproperties and the effects of rotational and translational input terms are separated out to faciliate the study of their contribution to the total response.

Numerical results are obtained for an example rotating machine. The applicability of the response spectrum approach is verified by a time history simulation study. The relative contributions of different terms to seismic response of the rotor-bearing system are also evaluated. It is observed that the contribution of the real eigenproperties of the system to the total response is negligible. It is also noted that the effect of the rotational excitations can be significant only if the intensities of the rotational input components at the base are very high. However, for a rotor sitting directly on the ground or on the floor of a supporting structure, the rotational inputs have only small effect on the response since such rotational excitations are usually not very strong in actual practice. Thus the rotational inputs can be ignored in the seismic analysis of such rotating machines. The rotational base inputs, however, can be considered, if desired, because the inclusion of the rotational components poses no difficulties in the proposed spectrum approach.

5.2 Suggested Future Research

In this research, the interaction between the rotating machine and its supporting structure was neglected when the auto and cross floor spectrum inputs to the machine were obtained. However, there is a possibility of a strong dynamic interaction between the machine and its supporting structure, especially if the machine is relatively heavy and tuned. The effect of an unbalnced rotating machine on the response of its supporting structure and the tuning between the machine frequency and the frequencies of the primary system can be very important. Also the axial loading due to seismic effects can be quite important in the design of some thrust bearings and axial stability analysis. Incorporation of the axial force in the analysis is a challenging problem which has not been explored. This topic can be studied further to achieve a better understanding of the behavior of rotating machines in a seismic environment.

Appendix A

Definition of System Matrices and Input Vector

The mass, damping and stiffness matrices and the forcing function of a rotor system in the finite element model are defined as follows:

$$[M] = \rho A \int_0^l [N_1]^T [N_1] ds + \rho I_x \int_0^l [N_2]^T [N_2] ds$$

$$[C] = \Omega I_p \int_0^l [N_2]^T (\{e_1\}\{e_2\}^T - \{e_2\}\{e_1\}^T)[N_2]^T ds + 2\rho A \int_0^l [N_1]^T [\omega][N_1] ds$$

$$\begin{aligned}[K] &= EI_x \int_0^l [N_2']^T [N_2'] ds + kGA \int_0^l [N_3]^T [N_3] ds \\ &\quad + \rho A \int_0^l [N_1]^T [\omega^2][N_1] ds + \rho A \int_0^l [N_1]^T [\dot{\omega}][N_1] ds\end{aligned}$$

$$\begin{aligned}\{f(t)\} &= -\rho A (\int_0^l [N_1]^T ds)\{a_b\} \\ &\quad - \rho A (\int_0^l [N_1]^T ds)[\dot{\omega}]\{e\} - \rho I_x (\int_0^l [N_2]^T ds)\{\ddot{\theta}_b\} \\ &\quad - \rho A (\int_0^l [N_1]^T ([\omega^2]\{e\} + [\omega]\{v_b\}) ds) \\ &\quad + \Omega I_p (\int_0^l [N_2]^T ds)(\{e_1\}\{e_2\}^T - \{e_2\}\{e_1\}^T)\{\dot{\theta}_b\}\end{aligned}$$

where $[N_1]$, $[N_2]$ and $[N_3]$ are the matrices of interpolation functions, $\{a_b\} = \{\dot{v}_b\} =$ vector of base acceleration, $\{\theta_b\} =$ vector of base rotation, $\{e_1\} = \{1,0\}^T$, $\{e_2\} = \{0,1\}^T$, $\{e\} = \{0, h, z_1 + s\}^T$ in which z_1 is the nodal coordinate, and

$$[\omega] = \begin{bmatrix} 0 & -\dot{\theta}_{zb} & \dot{\theta}_{yb} \\ \dot{\theta}_{zb} & 0 & -\dot{\theta}_{xb} \\ -\dot{\theta}_{yb} & \dot{\theta}_{xb} & 0 \end{bmatrix}$$

ρ, A, I_x, I_p, k, E and G are the physical and mechanical properties of the system, and Ω is the operating spinning speed of the shaft.

Appendix B

List of Constants in Seismic Wave Model

The coefficients of polynomials $L_i(\omega) = L_{i0} + L_{i2}\omega^2 + L_{i4}\omega^4$ and $N_i(\omega) = N_{i0} + N_{i2}\omega^2 + N_{i4}\omega^4 + N_{i6}\omega^6$ for calculating $[R_i]_l$ and the constants in equation (3.59) are listed as follows:

$$
\begin{aligned}
L_{10} &= \omega_j^2 \alpha_k \zeta_{11} \\
L_{12} &= (2\beta_j\omega_j - \alpha_k)\zeta_{11} + (2\beta_j\omega_j\alpha_k - \omega_j^2)\xi_{11} \\
L_{14} &= \xi_{11} \\
N_{10} &= \omega_j^2\omega_k^2\sigma_{11} \\
N_{12} &= (4\beta_j\beta_k\omega_j\omega_k - \omega_j^2 - \omega_k^2)\sigma_{11} + \omega_j^2\omega_k^2\nu_{11} + 2(\beta_k\omega_k\omega_j^2 - \beta_j\omega_j\omega_k^2)\varphi_{11} \\
N_{14} &= \sigma_{11} + (4\beta_j\beta_k\omega_j\omega_k - \omega_j^2 - \omega_k^2)\nu_{11} + 2(\beta_j\omega_j - \beta_k\omega_k)\varphi_{11} \\
N_{16} &= \nu_{11}
\end{aligned}
$$

$$
\begin{aligned}
L_{20} &= \omega_j^2 \alpha_k \zeta_{22} \\
L_{22} &= (2\beta_j\omega_j - \alpha_k)\zeta_{22} + (2\beta_j\omega_j\alpha_k - \omega_j^2)\xi_{22} \\
L_{24} &= \xi_{22}
\end{aligned}
$$

$$
\begin{aligned}
N_{20} &= \omega_j^2\omega_k^2\sigma_{22} \\
N_{22} &= (4\beta_j\beta_k\omega_j\omega_k - \omega_j^2 - \omega_k^2)\sigma_{22} + \omega_j^2\omega_k^2\nu_{22} + 2(\beta_k\omega_k\omega_j^2 - \beta_j\omega_j\omega_k^2)\varphi_{22} \\
N_{24} &= \sigma_{22} + (4\beta_j\beta_k\omega_j\omega_k - \omega_j^2 - \omega_k^2)\nu_{22} + 2(\beta_j\omega_j - \beta_k\omega_k)\varphi_{22} \\
N_{26} &= \nu_{22}
\end{aligned}
$$

$$
\begin{aligned}
L_{30} &= 0 \\
L_{32} &= (2\beta_j\omega_j\alpha_k - \omega_j^2)(\zeta_{12} - \zeta_{21}) - \alpha_k\omega_j^2(\xi_{12} - \xi_{21}) \\
L_{34} &= (\zeta_{12} - \zeta_{21}) + (\alpha_k - 2\beta_j\omega_j)(\xi_{12} - \xi_{21}) \\
N_{30} &= 0 \\
N_{32} &= \omega_j^2\omega_k^2(\varphi_{12} - \varphi_{21}) + 2(\beta_k\omega_k\omega_j^2 - \beta_j\omega_j\omega_k^2)(\sigma_{12} - \sigma_{21}) \\
N_{34} &= (4\beta_j\beta_k\omega_j\omega_k - \omega_j^2 - \omega_k^2)(\varphi_{12} - \varphi_{21}) + 2(\beta_j\omega_j - \beta_k\omega_k)(\sigma_{12} - \sigma_{21}) \\
&\quad +2(\beta_k\omega_k\omega_j^2 - \beta_j\omega_j\omega_k^2)(\nu_{12} - \nu_{21}) \\
N_{36} &= (\varphi_{12} - \varphi_{21}) + 2(\beta_j\omega_j - \beta_k\omega_k)(\nu_{12} - \nu_{21})
\end{aligned}
$$

where

$$
\begin{aligned}
\zeta_{rs} &= e_{rkm}z_{sjn} + e_{rkn}z_{sjm} \\
\xi_{rs} &= e_{rkm}a_{sjn} + e_{rkn}a_{sjm} \\
\sigma_{rs} &= z_{rjm}z_{skn} + z_{rjn}z_{skm} \\
\nu_{rs} &= a_{rjm}a_{skn} + a_{rjn}a_{skm} \\
\varphi_{rs} &= a_{rkn}z_{sjm} + a_{rkm}z_{sjn} - z_{rkn}a_{sjm} - z_{rkm}a_{sjn}
\end{aligned}
$$

$$
\mu_1^{rr} = \kappa_1\alpha_j - \frac{\kappa_2\alpha_j^3}{4c^2} + \frac{\kappa_3\alpha_j^2}{2c}
$$

$$
\begin{aligned}
\mu_2^{rr} &= \kappa_1\alpha_k - \frac{\kappa_2\alpha_k^3}{4c^2} - \frac{\kappa_3\alpha_k^2}{2c} \\
\mu^{cr} &= \frac{1}{2c^2}(U_2 + W_2) \\
\mu_1^{c} &= 4z_{1jm}z_{1jn} - \frac{a_{2jm}a_{2jn}\omega_j^4}{c^2} \\
\mu_2^{c} &= 4a_{1jm}a_{1jn} + \frac{z_{2jm}z_{2jn}}{c^2} - g_j a_{2jm}a_{2jn} + \frac{2\kappa_4}{c} \\
\mu^{cc} &= \frac{1}{c^2}(Y_{j2} + Y_{k2})
\end{aligned}
$$

$$\bar{U} = 2U_1 - \frac{1}{2c^2}(\alpha_k^2 U_2 - 2cU_3)$$

$$\bar{V} = 2V_1 - \frac{1}{2c^2}(\omega_j^4 W_2 - 2cV_3)$$

$$\bar{W} = 2W_1 + \frac{1}{2c^2}(V_2 - g_j W_2 + 2cW_3)$$

$$\bar{X}_j = 4X_{j1} - \frac{1}{c^2}(\omega_j^4 Y_{j2} - 2cX_{j3})$$

$$\bar{Y}_j = 4Y_{j1} + \frac{1}{c^2}(X_{j2} + 2cY_{j3} - g_j Y_{j2})$$

$$\bar{X}_k = 4X_{k1} - \frac{1}{c^2}(\omega_k^4 Y_{k2} - 2cX_{k3})$$

$$\bar{Y}_k = 4Y_{k1} + \frac{1}{c^2}(X_{k2} + 2cY_{k3} - g_k Y_{k2})$$

where

$$
\begin{aligned}
\kappa_1 &= (e_{1jm}e_{1kn} + e_{1jn}e_{1km})/(\alpha_j + \alpha_k) \\
\kappa_2 &= (e_{2jm}e_{2kn} + e_{2jn}e_{2km})/(\alpha_j + \alpha_k) \\
\kappa_3 &= (e_{1jm}e_{2kn} + e_{1jn}e_{2km} - e_{1km}e_{2jn} - e_{1kn}e_{2jm})/(\alpha_j + \alpha_k) \\
\kappa_4 &= a_{1jm}z_{2jn} + a_{1jn}z_{2jm} - z_{1jm}a_{2jn} - z_{1jn}a_{2jm}
\end{aligned}
$$

Appendix C

List of Constants in Correlation Matrix Model

The coefficients of polynomials $L'_i(\omega) = L'_{i0} + L'_{i2}\omega^2 + L'_{i4}\omega^4$ and $N'_i(\omega) = N'_{i0} + N'_{i2}\omega^2 + N'_{i4}\omega^4 + N'_{i6}\omega^6$ in equation (3.68) and the constant in equation (3.77) are listed as follows:

$$
\begin{aligned}
L'_{10} &= \omega_j^2 \alpha_k \zeta_{mm} \\
L'_{12} &= (2\beta_j\omega_j - \alpha_k)\zeta_{mm} + (2\beta_j\omega_j\alpha_k - \omega_j^2)\xi_{mm} \\
L'_{14} &= \xi_{mm} \\
N'_{10} &= \omega_j^2\omega_k^2\sigma_{mm} \\
N'_{12} &= (4\beta_j\beta_k\omega_j\omega_k - \omega_j^2 - \omega_k^2)\sigma_{mm} + \omega_j^2\omega_k^2\nu_{mm} \\
&\quad +2(\beta_k\omega_k\omega_j^2 - \beta_j\omega_j\omega_k^2)\varphi_{mm} \\
N'_{14} &= \sigma_{mm} + (4\beta_j\beta_k\omega_j\omega_k - \omega_j^2 - \omega_k^2)\nu_{mm} + 2(\beta_j\omega_j - \beta_k\omega_k)\varphi_{mm} \\
N'_{16} &= \nu_{mm}
\end{aligned}
$$

$$
L'_{20} = \omega_j^2 \alpha_k \zeta_{mn}
$$

$$
\begin{aligned}
L'_{22} &= (2\beta_j\omega_j - \alpha_k)\zeta_{mn} + (2\beta_j\omega_j\alpha_k - \omega_j^2)\xi_{mn} \\
L'_{24} &= \xi_{mn} \\
N'_{20} &= \omega_j^2\omega_k^2\sigma_{mn} \\
N'_{22} &= (4\beta_j\beta_k\omega_j\omega_k - \omega_j^2 - \omega_k^2)\sigma_{mn} + \omega_j^2\omega_k^2\nu_{mn} \\
&\quad +2(\beta_k\omega_k\omega_j^2 - \beta_j\omega_j\omega_k^2)\varphi_{mn} \\
N'_{24} &= \sigma_{mn} + (4\beta_j\beta_k\omega_j\omega_k - \omega_j^2 - \omega_k^2)\nu_{mn} + 2(\beta_j\omega_j - \beta_k\omega_k)\varphi_{mn} \\
N'_{26} &= \nu_{mn}
\end{aligned}
$$

$$
\begin{aligned}
L'_{30} &= (2\beta_j\omega_j\alpha_k - \omega_j^2)\zeta'_{mn} - \alpha_k\omega_j^2\xi'_{mn} \\
L'_{32} &= \zeta'_{mn} + (\alpha_k - 2\beta_j\omega_j)\xi'_{mn} \\
L'_{34} &= 0 \\
N'_{30} &= \omega_j^2\omega_k^2\varphi'_{mn} + 2(\beta_k\omega_k\omega_j^2 - \beta_j\omega_j\omega_k^2)\sigma'_{mn} \\
N'_{32} &= (4\beta_j\beta_k\omega_j\omega_k - \omega_j^2 - \omega_k^2)\varphi'_{mn} + 2(\beta_j\omega_j - \beta_k\omega_k)\sigma'_{mn} \\
&\quad +2(\beta_k\omega_k\omega_j^2 - \beta_j\omega_j\omega_k^2)\nu'_{mn} \\
N'_{34} &= \varphi'_{mn} + 2(\beta_j\omega_j - \beta_k\omega_k)\nu'_{mn} \\
N'_{36} &= 0
\end{aligned}
$$

where

$$
\begin{aligned}
\zeta_{mn} &= e_{km}z_{jn} + e_{kn}z_{jm} \\
\xi_{mn} &= e_{km}a_{jn} + e_{kn}a_{jm} \\
\sigma_{mn} &= z_{jm}z_{kn} + z_{jn}z_{km} \\
\nu_{mn} &= a_{jm}a_{kn} + a_{jn}a_{km} \\
\varphi_{mn} &= a_{kn}z_{jm} + a_{km}z_{jn} - z_{kn}a_{jm} - z_{km}a_{jn} \\
\zeta'_{mn} &= -e_{km}z_{jn} + e_{kn}z_{jm}
\end{aligned}
$$

$$\xi'_{mn} = -e_{km}a_{jn} + e_{kn}a_{jm}$$

$$\sigma'_{mn} = -z_{jm}z_{kn} + z_{jn}z_{km}$$

$$\nu'_{mn} = -a_{jm}a_{kn} + a_{jn}a_{km}$$

$$\varphi'_{mn} = a_{kn}z_{jm} - a_{km}z_{jn} - z_{kn}a_{jm} + z_{km}a_{jn}$$

$$\gamma_{mn} = \frac{2e'_{jm}e'_{kn}}{\alpha_j + \alpha_k}$$

References

1. Asmis, G. J. K. and Duff, C. G., 1978, 'Seismic Design of Gyroscopic Systems', ASME Paper 78-PVP 44, ASME/CSME *Pressure Vessel Piping Conference*, Montreal, Canada.

2. Burdisso, R. A. and Singh, M. P., 1987, 'Multiply Supported Secondary Systems, Part I: Response Spectrum Analysis', *Earthquake Engineering and Sructural Dynamics*, Vol. 15, pp. 53-72.

3. Clough, R. W. and Penzien, J., 1967, *Structural Dynamics*, Mcgraw-Hill Book Company, New York.

4. Earles, L. L., Papzzolo, A. B., Lee, C. K. and Gehold, C. H., 1987, 'Hybrid Finite Element-Boundary Element Simulation of Rotating Machinery Supported on Flexible Foundation and Soil', *Rotatory Machinery Dynamics*, ASME Design Technology Conference, Boston, MA, pp. 371-382.

5. Ghafory-Ashtiany, M. and Singh, M. P., 'Structural Response for Six Correlated Earthquake Components', *Earthquake Engineering and Structural Dynamics*, Vol. 14, pp. 103-109.

6. Hori, Y., 1988, 'Anti-Earthquake Considerations in Rotor Dynamics', *International Conference on Vibrations in Rotating Machinery*, Edinburgh, Proc. I.

Mech. E., pp. 1-8.

7. Iwatsubo, T., Kawahar, I., Nakagawa, N. and Kowai, R., 1979, 'Reliability Design of Rotating Machine Aagainst Earthquake Excitation', *Bulletin of the Japan Society of Mech. Engr.*, Vol. 22, No. 173, pp. 1632-1639.

8. Meirovitch, L., 1980, *Computational Methods in Structural Dynamics*, Sijthoff and Noordhoff, Alphen aan den Rijn, Netherlands.

9. Newmark, N. M., 1969, 'Torsion in Symmetrical Building', *Proc. 4th World Conference on Earthquake Engr.*, Santiago, Chile, 2, A.3, pp. 19-32.

10. Nigam, N. C. and Jennings, P. C., 1969, 'Calculation of response Spectra from Strong Motion Earthquake records', *Bull. Seism. Soc. Am.*, Vol. 59, pp. 909-922.

11. Rice, S. O., 1954, 'Mathematical Analysis of Random Noise', *Selected Papers on Noise and Stochastic Processes*, Dover Publications, New York.

12. Shinozuka, M., 1987, 'Stochastic Fields and Their Digital Simulation', *Stochastic Mechanics*, Vol. I, Columbia University.

13. Singh, M. P., 1980, 'Seismic Response by SRSS for Nonproportional Damping', ASCE, *Journal of Engineering Mechanics Division*, Vol. 106, No. 6, pp. 1405-1419.

14. Singh, M. P. and Burdisso, R. A., 1987, 'Multiply Supported Secondary Systems, Part II: Seismic Inputs', *Earthquake Engineering and Structural Dynamics*, Vol. 15, pp. 73-90.

15. Singh, M. P. and Chu, S. L., 1976, 'Stochastic Consderation in Seismic Analysis of Structures', *Earthquake Engineering and Structural Dynamics*, Vol. 4, pp. 295-307.

16. Singh, M. P. and Ghafory-Ashtiany, M., 1984, 'Structural Response under Multi-Component Earthquakes', ASCE *Journal of Engineering Mechanics Division*, Vol. 110, pp.761-775.

17. Singh, M. P. and Ghafory-Ashtiany, M., 1986, 'Modal Time History Analysis of Non-Classically Damped Structures for Seismic Motions', *Journal of Earthquake Engineering and Structural Dynamics*, Vol. 14, pp.133-146.

18. Soni, A. H. and Srinivasan, V., 1983, 'Seismic Analysis of a Gyroscopic Mechanical System', ASME *Journal of Vibration, Acoustics, Stress and Reliability in Design*, Vol. 105 pp. 449-455.

19. Srinivasan, V. and Soni, A. H., 1982, 'Seismic Analysis of Rotating Mechanical Systems—a Review', *Shock and Vibration Digest*, Vol. 14 No. 6, pp. 13-19.

20. Srinivasan, V. and Soni, A. H., 1984, 'Seismic Analysis of a Rotor-Bearing System', *Earthquake Engineering and Structural Dynamics*, Vol. 12, pp. 287-311.

21. Suarez, L. E., Singh, M. P. and Rohanimanesh, M. S., 1992, 'Seismic Response of Rotating Machines', *Earthquake Engineering and Structural Dynamics*, Vol. 21, pp. 21-36.